

Article

Evaluating the Forest Road Systems Subjected to Different Loadings by Using the Finite Element Method

Elena-Camelia Mușat *  and Ioan Bitir

Department of Forest Engineering, Forest Management Planning and Terrestrial Measurements, Faculty of Silviculture and Forest Engineering, Transilvania University of Brasov, Șirul Beethoven Street No. 1, 500123 Brasov, Romania

* Correspondence: elena.musat@unitbv.ro; Tel.: +40-761-646-361

Abstract: In the actual context, in which there is a trend of increasing the weight of the vehicles used to transport materials, checking the deformations of road systems as a response to dynamic and static loadings is necessary to better manage the road infrastructure. The goal of the study was to evaluate how the number and the thickness of layers, and the material types could influence the behavior of the road systems subjected to different loads, and to find out which of the road systems have the smallest deformations. The Romania forest roads are classified into three categories, and the most important are the principal forest roads. There were chosen road systems proper to this category. Consequently, nine types of road systems were considered, based on the materials used and the thickness of the layers, and the deformations were evaluated by considering loads of 25, 35 and 45 tons. For modeling the behavior of road systems under different loads, the Finite Element Method (FEM) was used taking into consideration the static domain. The models show that, in all the cases, the deformations depend on the number of layers, while the thickness of the ballast layer can reduce the deformations because of the rigidity of the structure. Those findings are very important because not all the modeled roads systems could provide suitable bearing capacity. Hence, an inappropriate thickness of the layers could negatively influence the behavior of road systems under the traffic with weight increased.

Keywords: forest roads; finite element method; road structure; loadings; truck; wood transport



Citation: Mușat, E.-C.; Bitir, I.

Evaluating the Forest Road Systems Subjected to Different Loadings by Using the Finite Element Method.

Forests **2022**, *13*, 1872. <https://doi.org/10.3390/f13111872>

Academic Editor: Kalle Kärhä

Received: 23 September 2022

Accepted: 7 November 2022

Published: 9 November 2022

Publisher's Note: MDPI stays neutral with regard to jurisdictional claims in published maps and institutional affiliations.



Copyright: © 2022 by the authors. Licensee MDPI, Basel, Switzerland. This article is an open access article distributed under the terms and conditions of the Creative Commons Attribution (CC BY) license (<https://creativecommons.org/licenses/by/4.0/>).

1. Introduction

The forest roads, like any other type of construction, undergo a series of structural changes as a result of use [1–4], which are closely related to the level of traffic at which were exposed [5–13]. Because of this, the sizing and the design are in a strong relation to future requests [5,12,14–17] and the materials used in construction [3,18–21], but also with the compliance or non-compliance of the proper conditions of the objective's exploitation and use [12,21–26].

Due to the importance that the forest roads have in providing accessibility to resources [27–30], balancing the harvests at spatial scale [31–34], supporting a sustainable forest management [32,35–38] and local communities [11,31,38–41], it becomes important to maintain them in a state that enables the efficiency and safety of transportation. Furthermore, they need to be planned by considering the forecasted traffic requirements [6,7,11,15,17,22,23,29,42], and are typically designed by including the costs of timber harvesting [34,43]. Nevertheless, the transportation activity has been found to have the greatest impact on the final price of the wood [1,44–49]. To balance the behavior of forest roads with the traffic, their design should be adapted to the constructive characteristics of the vehicles [22,23,50], particularly to their transportation capacity [11,51]. Practically, the bearing capacity of the roads has to overcome the additional loads from high-weight traffic [5–7,15–17,26,35].

In Romania, the forest roads are restricted to public traffic [4,15,52,53], and are classified into three categories (masterly, principal/main and secondary forest roads), depending on the traffic characteristics and the forested areas they serve [4,15,53]; accordingly, the road systems are usually selected based on the category of road [36]. In addition, most forest roads are made of flexible systems [20,54], which are sized based on the traffic requirements [11,15,17,55]. Gravel surfacing is the most common in Romanian forest roads [3,15,22–24,56], and most of the forest roads were designed for a maximum permissible weight of 25 tones [57], before 1990 [58]. The current regulations [15] take into consideration a maximum permissible weight of 38 tones, which is closer to the actual traffic requirements [11,59].

Due to the distribution of loads over the road surface, there is a high number of options which can be used to place the layers within a road system [3,17,60–63]. Undersized road systems are prone to premature failure [56], especially when the traffic occurs in the freezing / thawing periods [11,21,24,25], or during periods of high humidity [11,29,54,64]. It should be noted that the layers have different thicknesses and strengths and are made of materials whose quality may decrease with depth [8,9,54,56]. According to the literature [3,15], the upper layers should be made of stronger, high-quality materials [65–67]. The gravel pavements have to be well compacted, so that the entire road system be as impermeable as possible, which will prevent the action of climatic factors on the whole system. On the other hand, the layers' succession in terms of materials and thickness should provide a decrease in loading, so at the roadbed it will be less than the ground's load-bearing capacity [3,25,54,68].

Tracking the behavior of forest roads over time can provide useful information on the problems that arise due their overloading [12,13], standing for one alternative to propose improvements. However, it takes time, being difficult to track back the real traffic events and to conclude which management measures to be taken. To this end, a promising alternative is based on the simulation of road systems behavior under various traffic conditions. An important indicator in evaluating the behavior of road systems under different loads is the analysis of the contact between the wheel and the road [69–72], which depends on many factors, including the tire pressure, the type of vehicle, the number of axles and the distribution of loadings on axles, some aspects of interest in this regard is the shape of the contact trace between the wheel and the road [17], and the way in which the pressure is transmitted to the support surfaces, because the contact surface between wheel and road increase once with the loading on the entire vehicle and the loading of each axle in part [70].

Each vehicle that passes on a road induces in the structure an impulse which tends to deform the road system. Until a loading level, the stress is supported by the structure's layers because of the elastic behavior, but during the time, the road systems progressively deform as a consequence of traffic, as number and type of vehicles, loadings and weather conditions [67,69]. This residual deformation could be bigger when the road's layers are too thin and composed of improper materials, being a risk for rutting formation [67]. Taking into consideration all these possibilities, some researchers tried to estimate the behavior of road systems by using different software, like Finite Element Method, which was improved along the time [73].

The Finite Element Method (FEM) has been used in various fields of engineering, including in modeling the behavior of road systems [8,9,60,61,64,74–76]. In order to simulate the effect of traffic on road systems, many authors have resorted to the Finite Element Method, also applied in the case of the present research, either to analyze the stress and deformations occurring in the case of roads with non-rigid road systems [59,71–73], or to determine the number of load cycles that asphalt roads can withstand [8,9,60,77], and to observe the impact of multi-axle vehicles on road systems [17,61,67,78], even to highlight the differences that appear in the case of displacements in the depth of road systems with or without geogrids, at various test cycles [68,71]. These interactions can be analyzed both in the static and dynamic domain [11,54,60,61], while understanding the influence of traffic on the support surfaces is essential both for the design of resistant transport ways, as well

as to be able to evaluate, later in use, the factors that influence the behavior of constructions over time [2,72].

The Finite Element Method has not been used to model the behavior of non-rigid forest road systems with three and four layers under different loads in static domain, so the present study is focused on it. The goal of the study was to evaluate how the number and the thickness of layers, and the material types could influence the behavior of the road systems subjected to different loads, and to find out which of the road systems have the smallest deformations. In order to achieve the proposed goal, the following objectives have been set: (i) to establish standard types of road systems characteristic for the roads with an annual traffic between 5000 and 50,000 tons per year (known as principal roads in Romania); (ii) to make a numerical evaluation of road layers by using the Finite Element Method; (iii) to evaluate which one of the modeled road systems could provide a suitable behavior under loads that exceed the maximum permissible weight.

2. Materials and Methods

2.1. Forest Road Systems Taken into Consideration

As was mentioned before, in Romania, the forest roads are classified into three categories [15], and the principal/main roads represent almost a quarter of them [34], and the wood which is transported on secondary forest roads pass on main roads. Those roads were sized and designed to serve from 1000 to 10,000 ha and to support annual traffic between 5000 and 50,000 tons [4,15], at a speed of 20–25–40 km/h. Besides that, the majority of Romanian forest roads were built before 1990 with a maximum permissible weight of 25 tons [57], smaller than 38 tons, which is the limit nowadays. Therefore, the majority of the forest roads are degraded and have to be reconstructed [4] to support the increased weight.

This is the reason in order to run the simulations, three types of road systems were selected as being suitable for the main forest roads (Table 1), according to the forest road design regulations [15]. For each type three variants by sizing the thickness of the ballast layer were studied at 200, 300 and 400 mm, respectively. Each model of road system was studied in three loading situations of the vehicle, respectively for 25, 35 and 45 tons, resulting in nine road systems and 27 calculation models.

Table 1. The evaluated road systems as component layers, materials and thickness.

Road System Type	Layer's Thickness [mm] and the Modulus of Elasticity [MPa]							
	Mixed Crushed Stone [mm]	Crushed Stone, Assortment 63/90 [MPa]	Crushed Stone, Assortment 63/90 [mm]	Pitching of Crushed Stone [MPa]	Pitching of Crushed Stone [mm]	Ballast Layer [mm]	Ballast Layer [MPa]	
I.1	120	500	150	400	100	300	200	152
I.2	120	500	150	400	100	300	300	182
I.3	120	500	150	400	100	300	400	208
II.1	120	500	-	-	150	300	200	152
II.2	120	500	-	-	150	300	300	182
II.3	120	500	-	-	150	300	400	208
III.1	100	300	-	-	250	300	200	152
III.2	100	300	-	-	250	300	300	182
III.3	100	300	-	-	250	300	400	208

For the crushed stone it was considered the basalt, as a volcanic rock, a hard rock, very resistant to traffic, compact, with a fine grain, characteristics which make it suitable for surfacing layer [65,79,80]. Instead, the ballast layer, even if is a moderately hard and durable sedimentary rock, is not so resistant to traffic, being more suitable for base layer [81].

The choosing of those stony materials in the road system was based on the recommendations from the literature, where it is mentioned that the most resistant materials have to be placed in the upper part of the structure and the materials with decreased quality and

resistance have to be placed in the base layers [3,66,67], because the surfacing layers and the materials from their composition must be durable under different conditions of traffic and weather, well graded and mechanically stable [65].

In Table 1 were presented the layer's thickness, considered after the compaction up to 95%, because the density is strongly related to the compaction and humidity. For modelling, it was considered that the road system is dry and the Poisson coefficient, which is used to quantify the stiffness stress of the materials [70], was 0.27 for each stony layer. The subgrade was considered by gravel with sand, with a plasticity index smaller than 10%, a Poisson coefficient of 0.42, and a modulus of elasticity of 70 MPa [15,53].

2.2. The Use of FEM in Evaluating the Behavior of Road Systems

In order to determine the states of displacement and the remaining deformations of the road system under the actions of the loadings, the Finite Element Method was used, the calculations being performed in the static linear domain, considering that the deformations increase progressively from zero to a real value and remain constant. To simulate the road system deformation, a test sector of a forest road with the dimensions of $5 \times 2 \times 2$ (length \times width \times thickness)[m] was modeled (Figure 1).

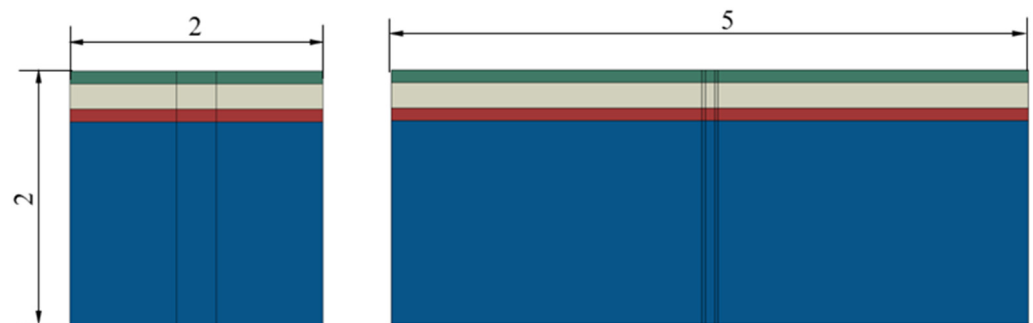


Figure 1. Dimensions [m] of the considered road test section (ballast layer—blue color, pitching of crushed stone—red, crushed stone, assortment 63/90—gray, mixed crushed stone—green).

Figure 2a,b shows the finite element discretized models for three principal road systems with three and four layers, using the Abaqus CAE technical calculation program; the same program being used by Leonardi and his collaborators [76], Calvarano and his collaborators [71] and Karadag and his collaborators [72]. The 3D finite elements of the hexahedron type simulated the layers of the road system based on the material properties assigned to each layer. The connection between the layers of the pavement was made by the common nodes between the finite elements.

For the application of the Finite Element Method, the considered road layers were fixed, in all directions, on the embankment, and the loading force was applied to the equivalent contact surface between the wheel and the surfacing layer (Figure 3), considering a speed of 25 km/h. The main forest roads were designed for speed between 20 and 40 km/h. Even so, the recommended speed for traveling, specified in the Romanian forest road design normative, is 25 km/h [15].

Using the Finite Element Method, it was followed how bigger is the deformation of the road pavement on the direction of pressure, taking into account the results obtained for each wheel, corresponding to each axle.

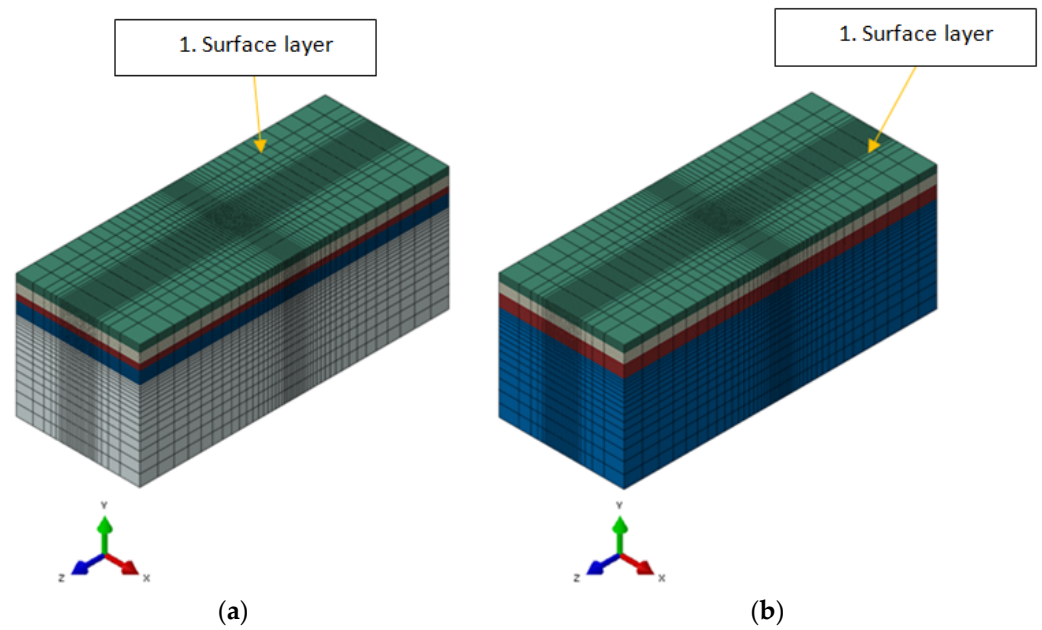


Figure 2. Hexahedron finite element models: (a). for the first type of road system; (b). for the second and the third type of the road systems.

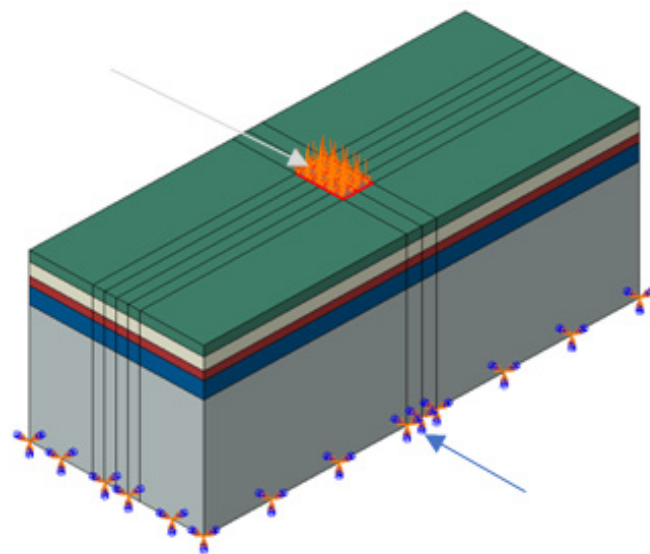


Figure 3. Boundary conditions.

2.3. The Vehicle and Loads Characteristics

For the comparative study, three loads were considered, which were assumed to be distributed on the axles of a known truck (Table 2), namely ATF 25 (Figure 4). This type of vehicle is commonly used for design of the forest road pavements in Romania [15].

Table 2. Loading distribution on each axle of the ATF 25 truck.

Truck Payload [tons]	Front Axle Loading [tons]	Rear Axles Loading of the Tractor [tons]	Loading on Semi-Trailer Axles [tons]
25	3.750	10	11.250
35	5.250	14	15.750
45	6.750	18	20.250

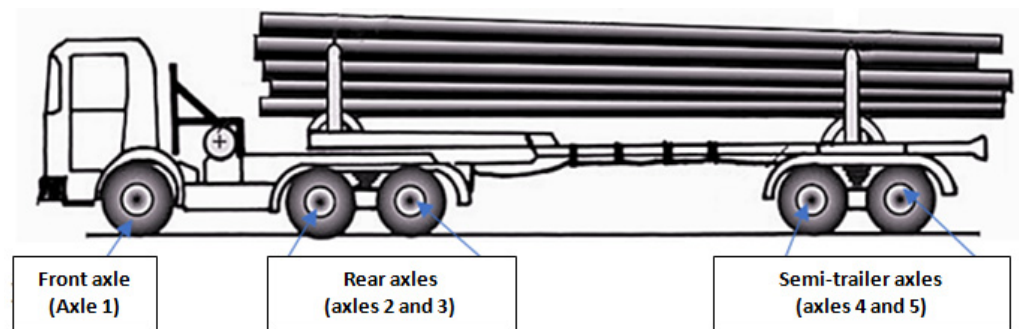


Figure 4. The axles of ATF 25 truck.

When the vehicle travels on the road, the structure deforms, causing the settlement of the layers. After the passing of each axle, the road system relaxes, and even if this relaxation extends up to the subground, each layer keeps a residual deformation. The total loading produced by each axle was distributed on each wheel, in order to obtain the deformation of the road pavement, which comes into contact with each wheel at a given time. Thus, it could be estimated which was the remaining deformation of the road pavement after passing the vehicle with a given payload.

The contact area between the wheel and the road was calculated on the basis of tire size and wheel pressure, thus determining an equivalent contact area, which could be expressed by multiplication of the uniform pressure at the surfacing layer, in MPa, with the diameter of the equivalent circle of contact, in mm [15]. The corresponding load of each wheel on the front and rear axles, as well as of the semi-trailer axles, was applied to this equivalent contact surface. Figure 5 shows the equivalent contact surfaces between the vehicle wheel and the road, corresponding to a front wheel and a rear wheel of the truck, respectively.

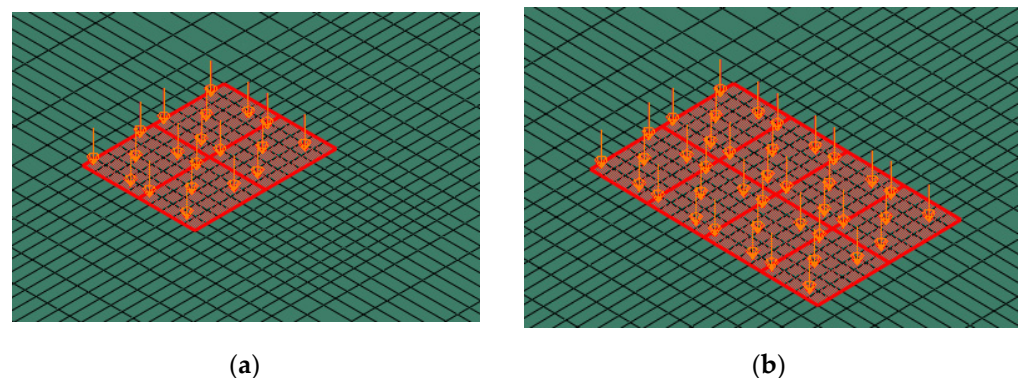


Figure 5. Force application area: (a). for a front wheel; (b). for the double wheels of the rear axle of the tractor.

Figure 6 shows the variation of loadings on each wheel. The displacements and deformations have been calculated for a total load of 25, 35 and 45 tons respectively, distributed over the entire vehicle, in the calculation being considered half of it, due to its constructive symmetry. The force was distributed on each wheel in relation to the maximum load of 40 tons.

For each model, it was determined:

- The maximum deformation of the surfacing layer after the passage of each wheel;
- The displacement into the depth of the entire road system after passing the vehicle;
- The residual deformation after the passage of the vehicle.

In order to highlight the differences between the nine road system types and 27 models of calculation, a comparative study was performed for the maximum and the residual

deformations obtained on the contact surface between the road and the wheel. So, the comparative study followed the state of deformation of the entire system during traffic, when the maximum loading force stress the surfacing layer, and the state of residual deformation, when the vehicle has left the road.

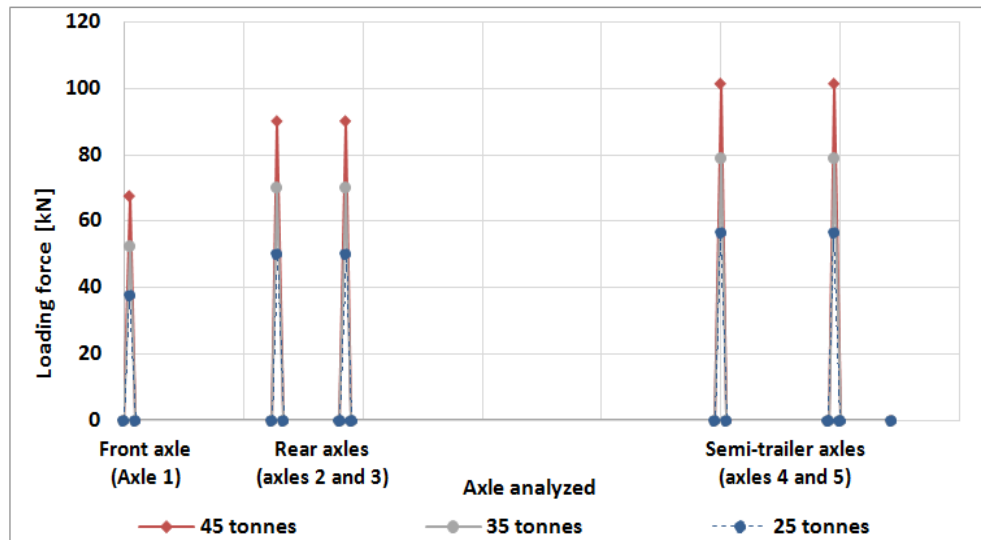


Figure 6. Distribution of loadings on each axle at ATF 25 truck.

3. Results

3.1. Residual Deformation Distribution and Vector Distribution of Residual Deformations

Figure 7 shows the distribution of the surfacing layer deformation, after passing the front wheels (single axle—Figure 7b), and after passing all the wheels (Figure 7c), in the direction of loading on pavement. The residual deformations obtained after passing all the axles are indicated in Figure 8, results corresponding to a single pass of the vehicle, with a speed of 25 km/h.

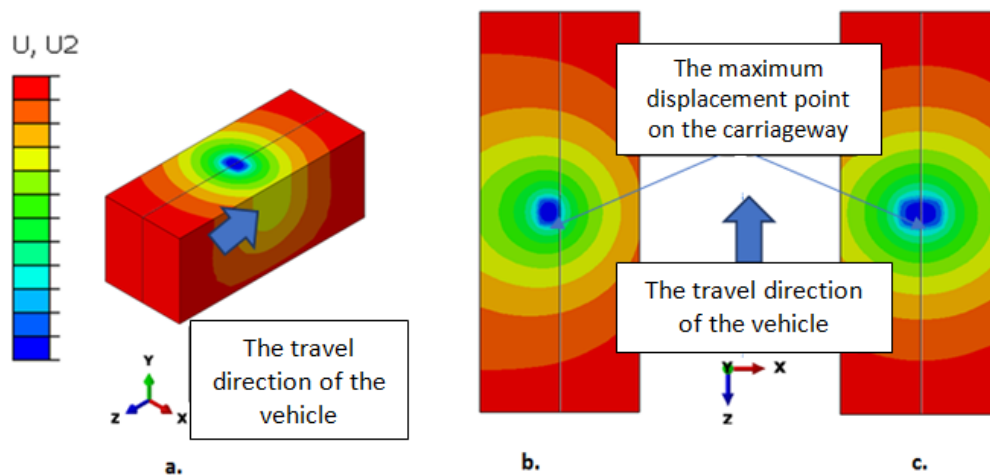


Figure 7. General view of the distribution of deformations: (a). an isometric view of the road; (b). the distribution of deformations after passing the front axle; (c). the distribution of the deformations after the passing of all the axles.

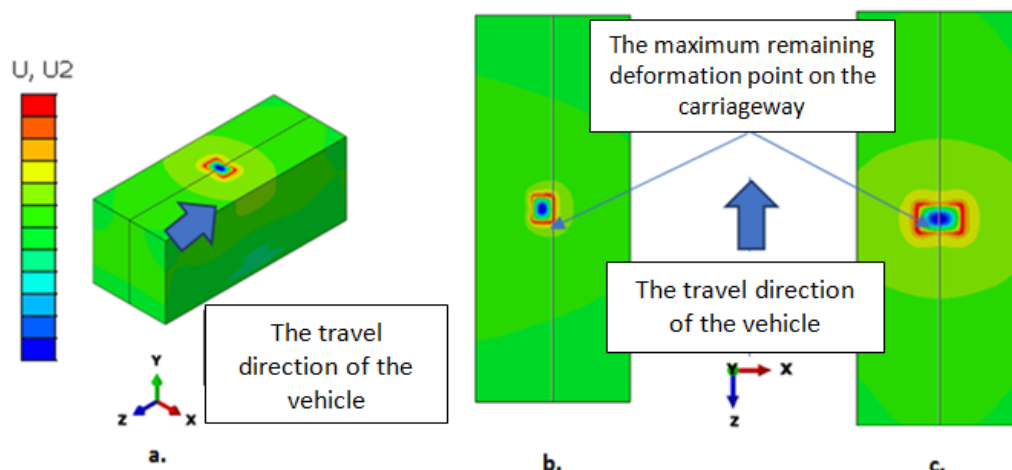


Figure 8. General view of the distribution of residual deformations: (a). an isometric view of the road; (b). the distribution of residual deformations after passing the front axle; (c). the distribution of the residual deformations after the passing of all the axles.

The residual deformation maintained in the road system after the passing the load can be seen in Figure 9. The vectors of the residual deformations have a positive direction on the outside of the pressed surface, but in the pressing area the vectors have a negative direction, which indicates the compaction of the road. This type of deformation, left after the passage of the vehicle, can lead to the formation of ruts. The distribution of the color spectrum of the total deformations, as well as of the residual ones, is identical for all the studied structures types, the difference between them being the numerical value of the deformations. As it can be seen in Figures 7–9, for each degree of deformation a different color was used. Taking into consideration that the biggest pressure was applied in the center of the contact area between wheel and surfacing layer, at the same point the highest deformations were obtained, symbolized here with dark blue color. Once with increasing of the distance from this central point, the deformations become smaller and the colors change from light blue to green, yellow and red (area where the deformations are very low and the structure has an elastic behavior).

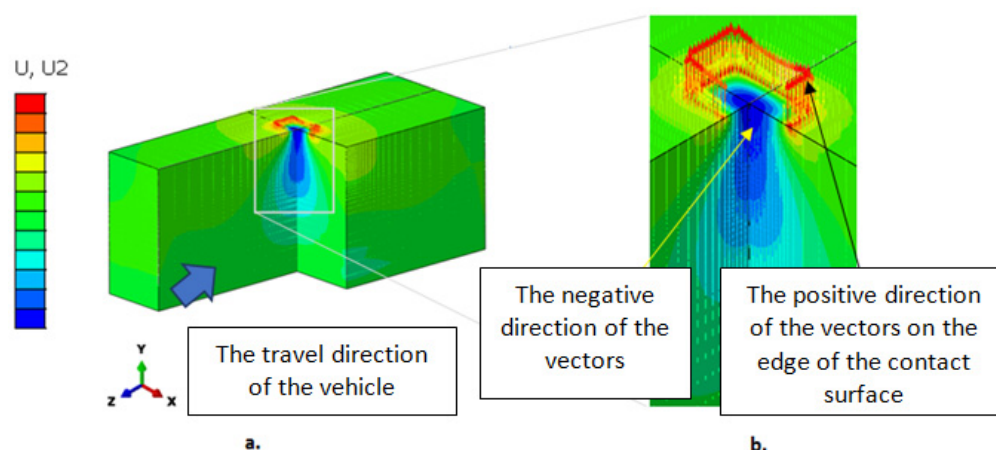


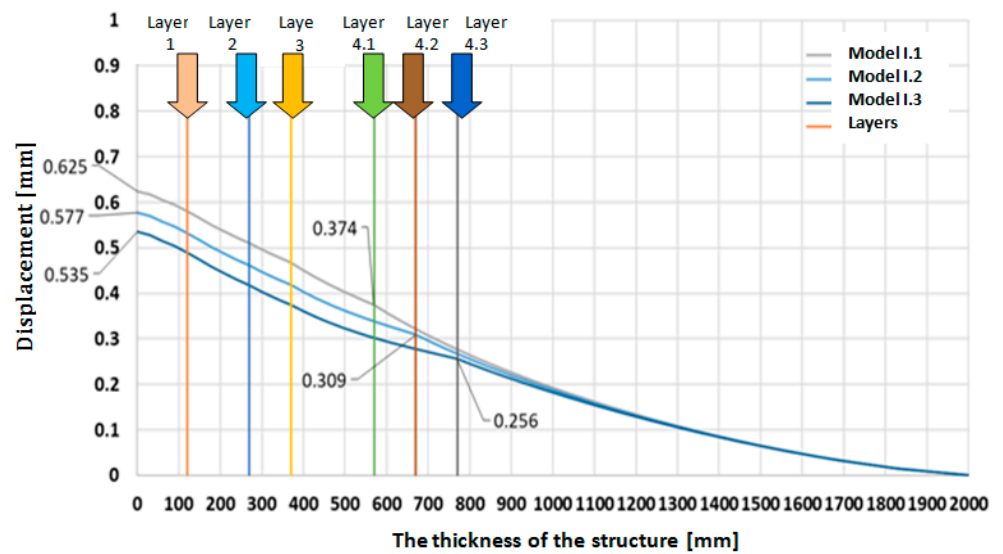
Figure 9. Depth section of the road—Vector distribution of the remaining deformations: (a). an isometric view of the road; (b). the distribution in deep of the remaining deformations after passing of all the wheels.

3.2. Numerical Evaluation of Deformations in the Case of Typical Road Structures

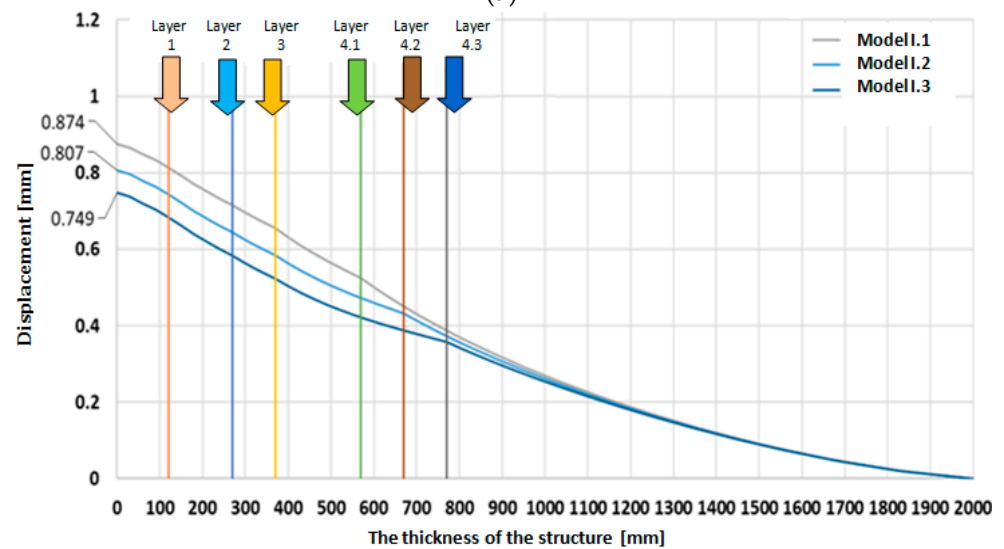
3.2.1. The Displacement of Structure's Layers in Depth

Type I of Road Systems

The displacements of the layers in depth, recorded for the type I of road systems tested at 25, 35 and 45 tons, indicate a higher rigidity of the I.3 variant, characterized by a thicker ballast layer on the embankment (400 mm), as opposed to variants I.1 and I.2 (200 and 300 mm). Related to the displacements in the depth, it was found that they vary between 0.625–0.653 mm when the road systems are tested at 25 t, between 0.874–0.749 mm at loads of 35 t, and between 1.124–0.963 mm at loads of 45 t (Figure 10a–c), so the increase in load places more stress on the road systems, the displacements of the layers into the depth being greater with the increase in pressure and the decrease in the thickness of the ballast layer placed on the embankment.

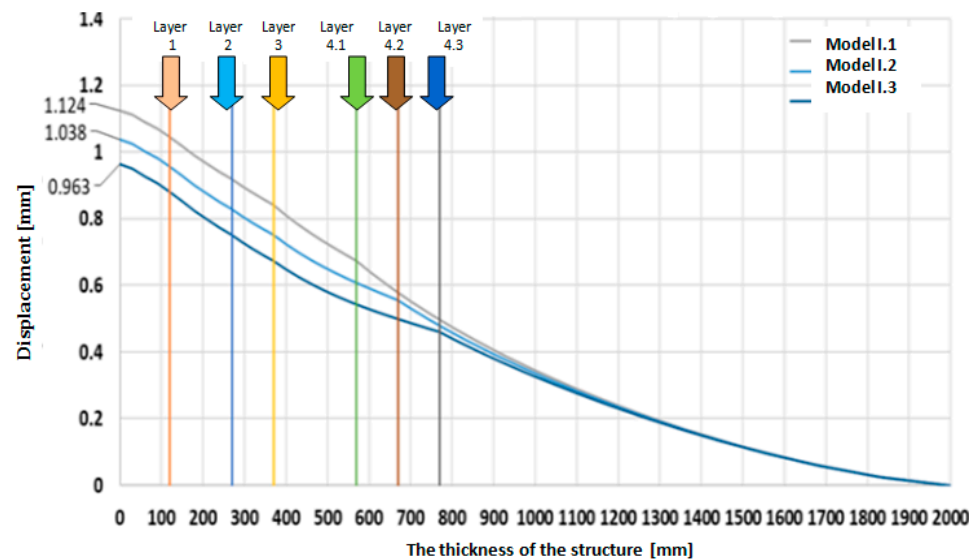


(a)



(b)

Figure 10. Cont.



(c)

Figure 10. The displacements into the depth recorded at type I of road systems subjected at 25 tons (a), 35 tons (b) and 45 tons (c).

Type II of Road Systems

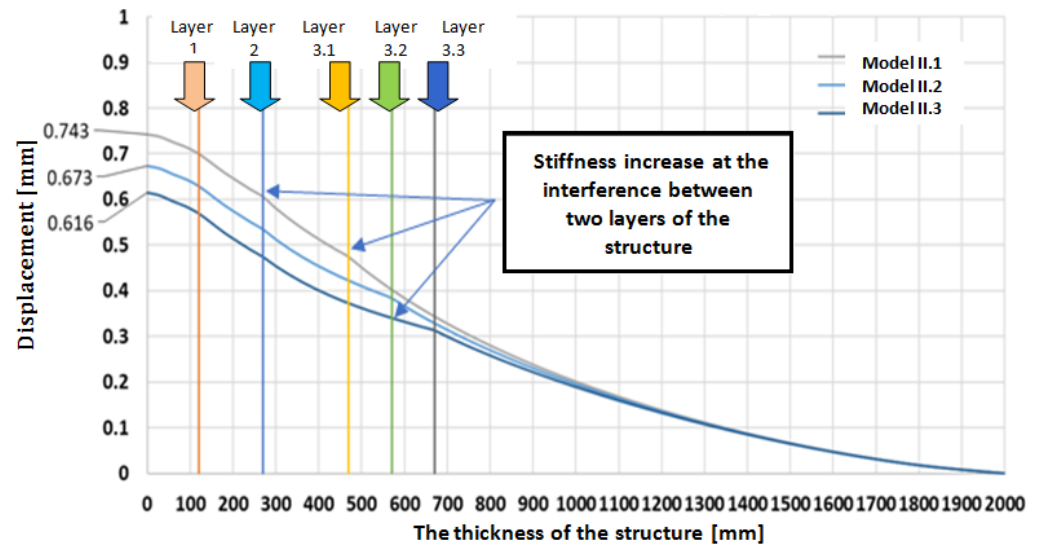
In the case of type II road systems, it is observed, once again, that the greater thickness of the ballast layer on the embankment leads to a greater stiffness of the type II.3 road system, regardless of the loading level (25, 35 or 45 tons). In addition, an increase in stiffness is observed between layers 2 and 3, which can be attributed to the materials used in the type II forest road systems compared to type I. Thus, they consist of three layers, with a thickness of 370 mm, to which the ballast layer of 200 mm (I.1), 300 mm (I.2) or 400 mm (I.3) is added, in time, that type II road systems consist of two layers, 270 mm thick, to which the ballast layer is added (200, 300 or 400 mm), which means that the optimal mix ballast layer (100 mm) and the broken stone sort 63/90 (150 mm), which are part of type I road systems, play an important role in reducing the displacement of layers in depth. For type II, the displacements in depth vary between 0.743–0.616 mm when they are loaded at 25 t, between 1.040–0.862 mm when they are loaded at 35 t, and between 1.337–1.108 mm at loads of 45 t (Figure 11a–c).

Type III of Road Systems

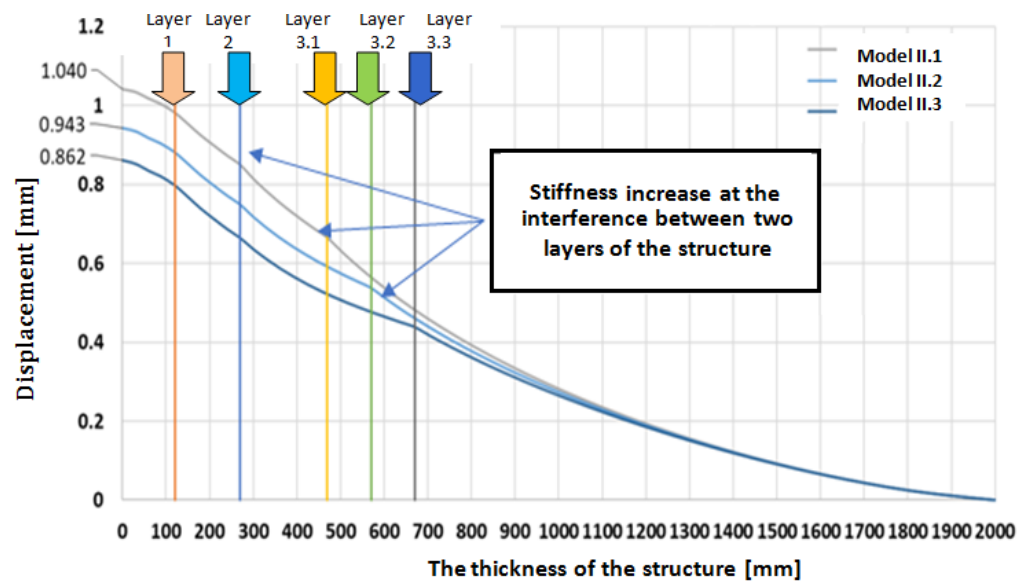
Compared to the displacement of the layers into the depth for type III road systems, a reduction in them is found, as well as an increased rigidity of the III.3 structure, conferred by the thicker ballast layer. In addition, the same increase in stiffness between layers 2 and 3, found in the case of type II road systems, is noted, which draws attention to the rough stone blocking layer which, regardless of thickness (150 mm—type II, and 250 mm—type III), confer properties similar to type II and III road systems, the values obtained for displacements being very close in those two situations. The recorded displacements ranged from 0.737–0.632 mm for 25 t loads, between 1.031–0.885 mm for 35 t loads, and between 1.326 and 1.138 for 45 t loads (Figure 12a–c).

Comparatively analyzing the displacement of the layers into the depth for the three types of road systems, with their own variants (Table 3), it was found that the values obtained for type II and III are relatively close and much higher than those obtained following the application of type I road systems, consisting of three layers, with a thickness of 370 mm, to which the layer of ballast is added (200, 300 or 400 mm). The lack of a layer in the structure, as happen in the case of types II and III, consisting of two layers (270 mm and 350 mm), to which the layer of ballast is added on the embankment (200, 300 or 400 mm),

has a significant impact in increasing the value of displacements into the depth, values that rise with the increase in the pressure level (25, 35 or 45 t), but also with the reduction in the thickness of the ballast layer (400–300–200 mm).

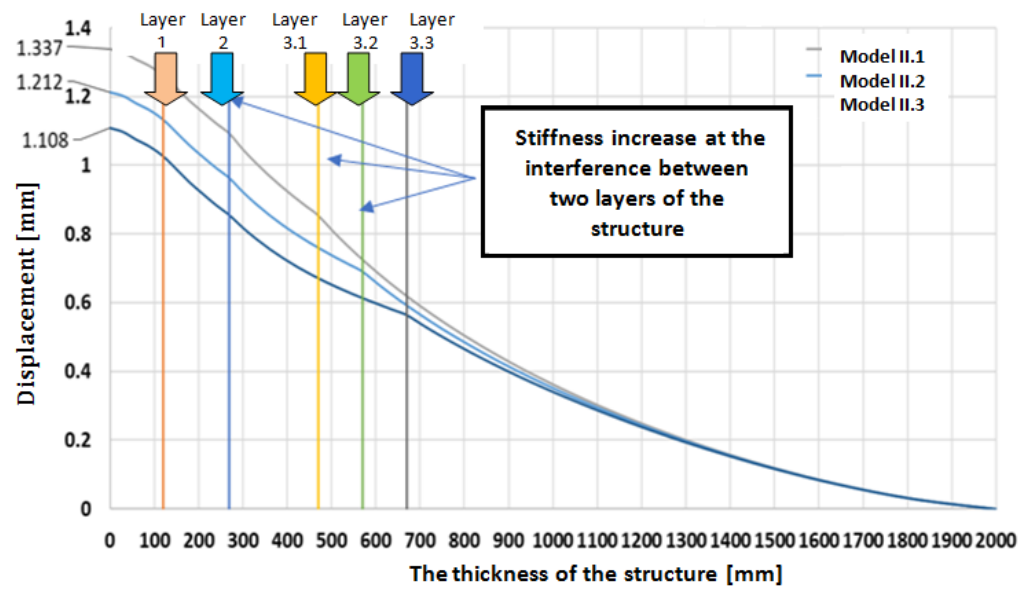


(a)



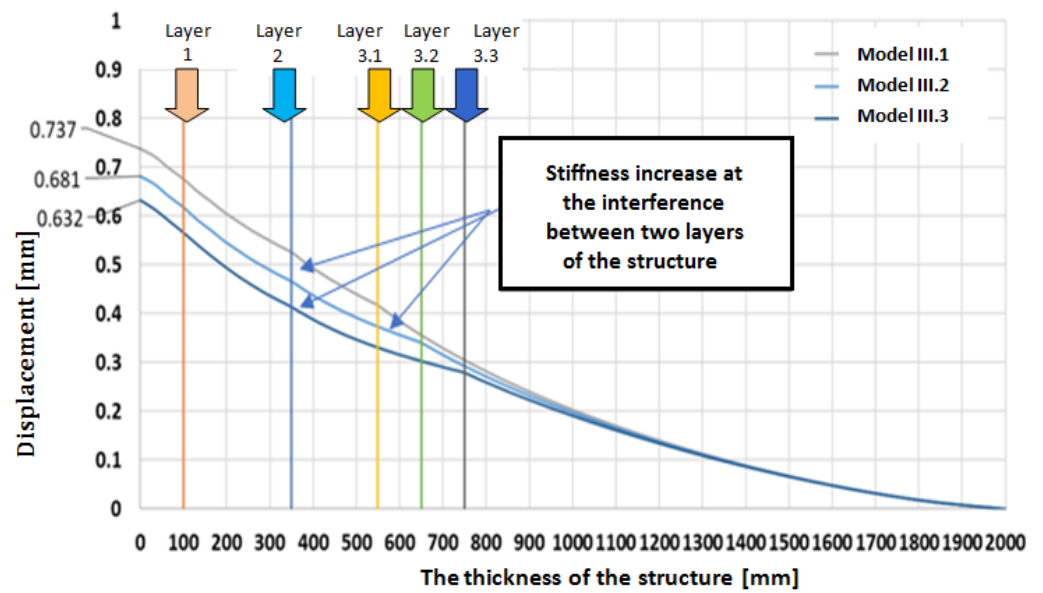
(b)

Figure 11. Cont.



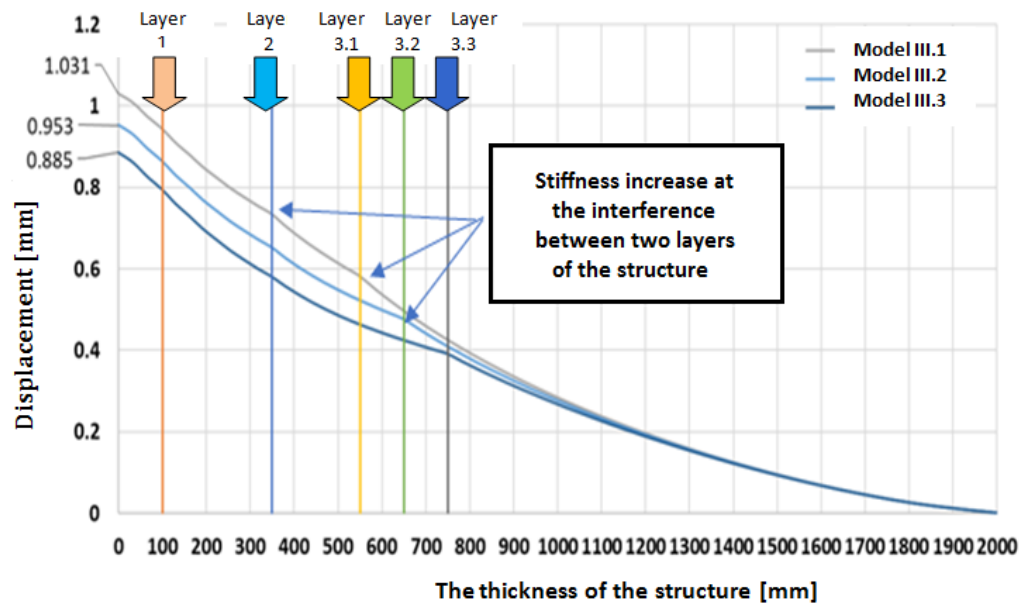
(c)

Figure 11. The displacements into the depth recorded at type II of road systems subjected at 25 tons (a), 35 tons (b) and 45 tons (c).

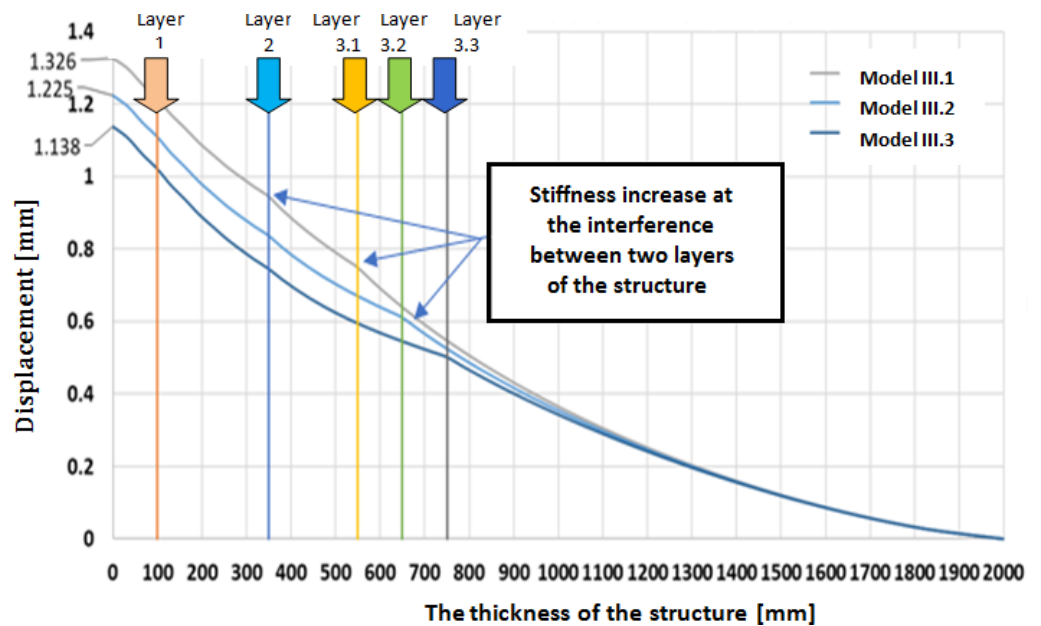


(a)

Figure 12. Cont.



(b)



(c)

Figure 12. The displacements into the depth recorded at type III of road systems subjected at 25 tons (a), 35 tons (b) and 45 tons (c).

On the other hand, analyzing the materials that enter in the composition of analyzed road systems and the number of layers, it was found that types II and III were similar in terms of layers and component materials, while types I and III road systems were similar in terms of the entire structure’s thickness. However, the layers of broken stone sort 63/90 (150 mm) and optimally mixed ballast (100 mm), which are part of type I road systems, give them better resistance to stress, the displacements into the depth being less in the case of these structures, probably due to the better wedging between the stony materials.

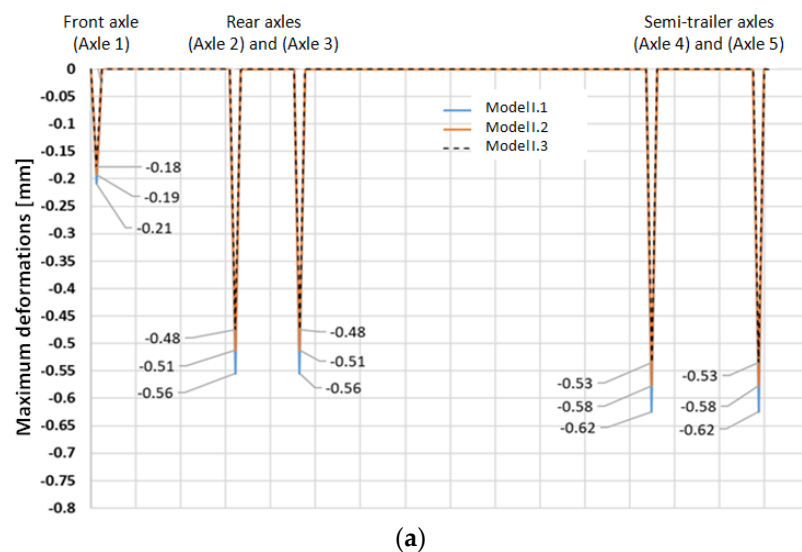
Table 3. The displacements into the depth of layers recorded at 25, 35 and 45 tons.

Loading [tons]	25 tons			35 tons			45 tons		
Type of structure	I.1	I.2	I.3	I.1	I.2	I.3	I.1	I.2	I.3
Displacement [mm]	0.625	0.577	0.535	0.874	0.807	0.749	1.124	1.038	0.963
Type of structure	II.1	II.2	II.3	II.1	II.2	II.3	II.1	II.2	II.3
Displacement [mm]	0.743	0.673	0.616	1.040	0.943	0.862	1.337	1.212	1.108
Type of structure	III.1	III.2	III.3	III.1	III.2	III.3	III.1	III.2	III.3
Displacement [mm]	0.737	0.681	0.632	1.031	0.953	0.885	1.326	1.225	1.138

3.2.2. The Maximum Deformations Recorded at 25, 35 and 45 Tons Loadings Type I Road Systems

In the case of type I road systems (Figure 13a–c) it was found that the maximum deformations vary both with the ballast layer's thickness on the embankment and with the increase in pressure, noting that the maximum deformations differ depending on the axle taken into consideration. Thus, for the front axle of the truck, the maximum deformations vary from 0.18 mm (I.3—25 t) to 0.37 mm (I.1—45 t), for the rear axles it oscillates from 0.48 mm (I.3—25 t) and 1.00 mm (I. 1—45 t), and for the semi-trailer axles, from 0.53 mm (I.3—25 t) to 1.12 mm (I.3—45 t). These values highlight, once again, the impact that the ballast layer's thickness at the embankment level has on the deformations, with greater deformations being recorded in the case of road systems with a lower thickness of this layer (I.1 and I. 2) and smaller deformations if the ballast layer has the maximum thickness considered in the present analysis (400 mm), which gives the structure greater rigidity and better behavior under loading pressure.

In addition, a progressive increase in deformations was observed with increasing of pressure level. Thus, for the front axle, there are differences of 0.03 mm between the considered road systems variants (I.1., I.2 and I.3) tested at 25 t, of 0.04 mm at 35 t and 0.05 mm for loadings of 45 t. For the rear axle, the values vary by up to 0.08 mm for the 25 t loads, by 0.11 mm for the 35 t loads, and by 0.14 for the 45 t loads. For the semi-trailer axles, greater differences were found between the maximum deformations, in relation to the type of road system and the load, these being 0.09 mm for 25 t, 0.12 mm for 35 t and 0.16 mm for 45 t loads.

**Figure 13.** Cont.

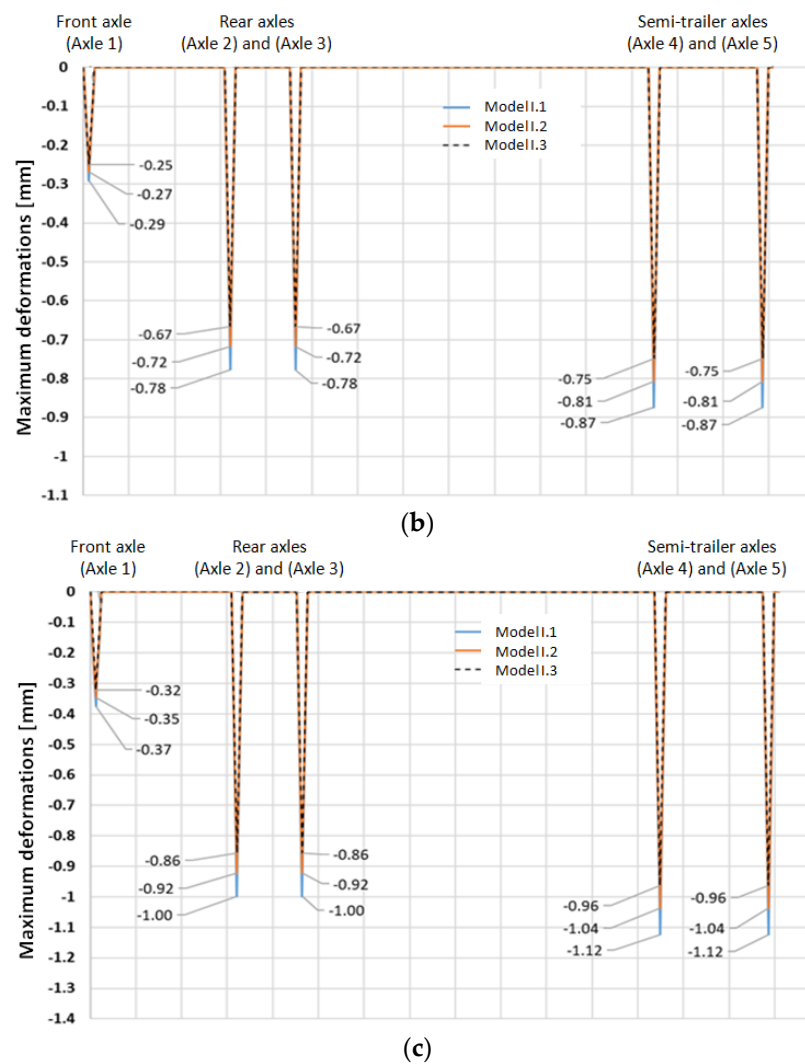


Figure 13. The maximum deformations recorded at type I road systems loaded at 25 tons (a), 35 tons (b) and 45 tons (c).

Type II Road Systems

As in the case of type I road systems, in the case of type II (Figure 14a–c) it was found that the values of the maximum deformations vary with the axle that passes over the support surface, but also with the level of pressure, and being reducing to greater thicknesses of the road system. Compared to the variation in values, it was observed that the maximum deformations oscillate for the front axle between 0.21 and 0.25 mm at 25 t, between 0.25 and 0.35 mm at 35 t and between 0.37 and 0.45 mm at 45 t loads. The upward trend was also preserved in the case of double axles, the highest values being registered at the rear axle, when the maximum deformations are 1.34 mm for road system II.1, 1.21 mm for type II.2 and 1.11 mm for II.3, which highlights once again the fact that a greater thickness of the ballast layer on the embankment gives the structure greater rigidity, behaving better under loading pressure.

Type III Road Systems

The tendency to increase the maximum deformations with the increase in the loading level was also found in the case of type III road systems (Figure 15a–c). There were significant differences between the values recorded at the front axle of the truck compared to the two double axles, the values being 3 times higher. Thus, the maximum deformations oscillate between 0.21 mm (III.3—25 t) and 0.44 mm (III.1—45 t) for the front axle, between

0.56 mm (III.3—25 t) and 1.18 mm (III.1—45 t) for the rear axles, and between 0.63 mm (III.3—25 t) and 1.33 mm (III.1—45 t) for the semi-trailer’s axles.

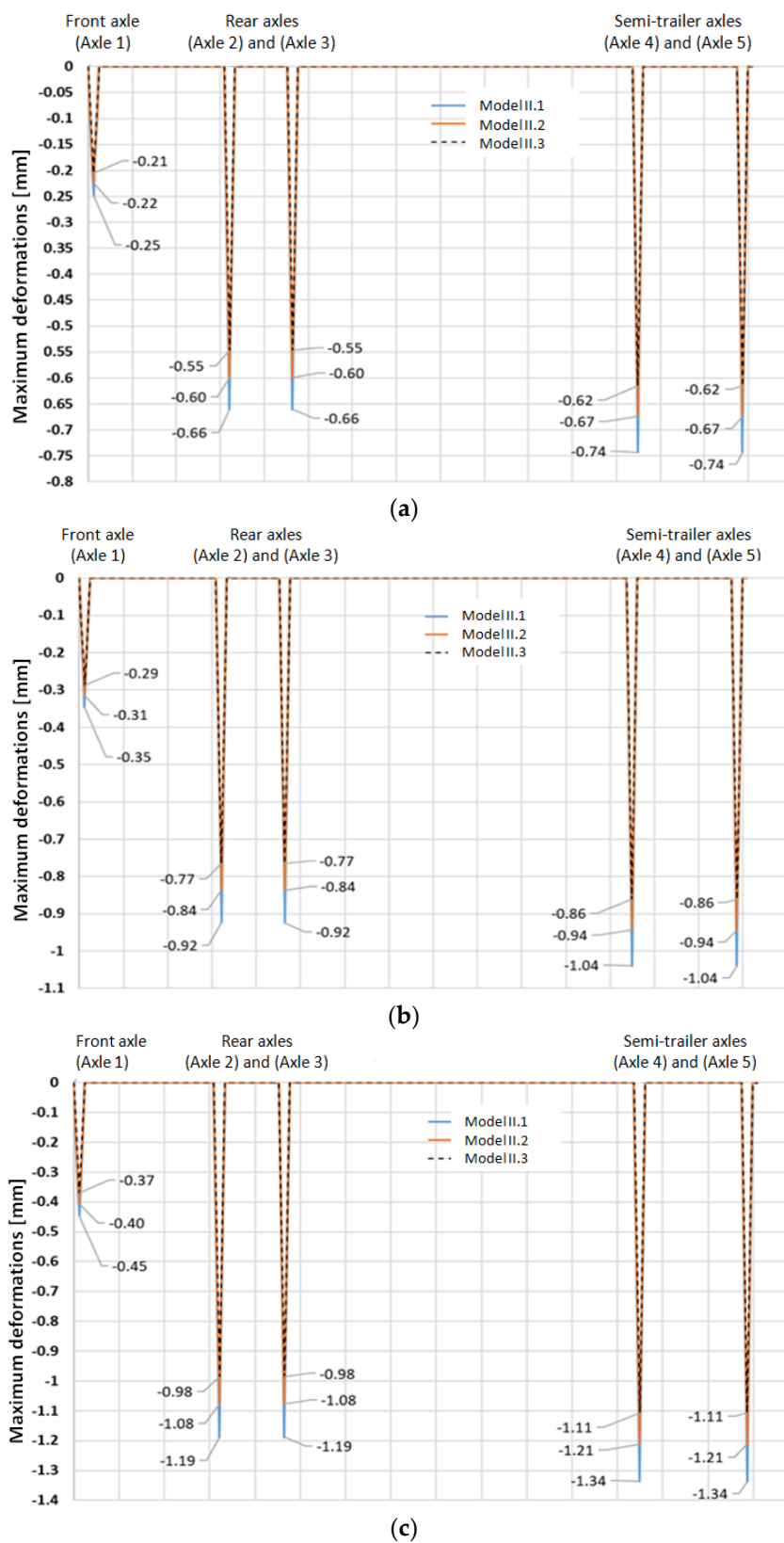


Figure 14. The maximum deformations recorded at type II road systems loaded at 25 tons (a), 35 tons (b) and 45 tons (c).

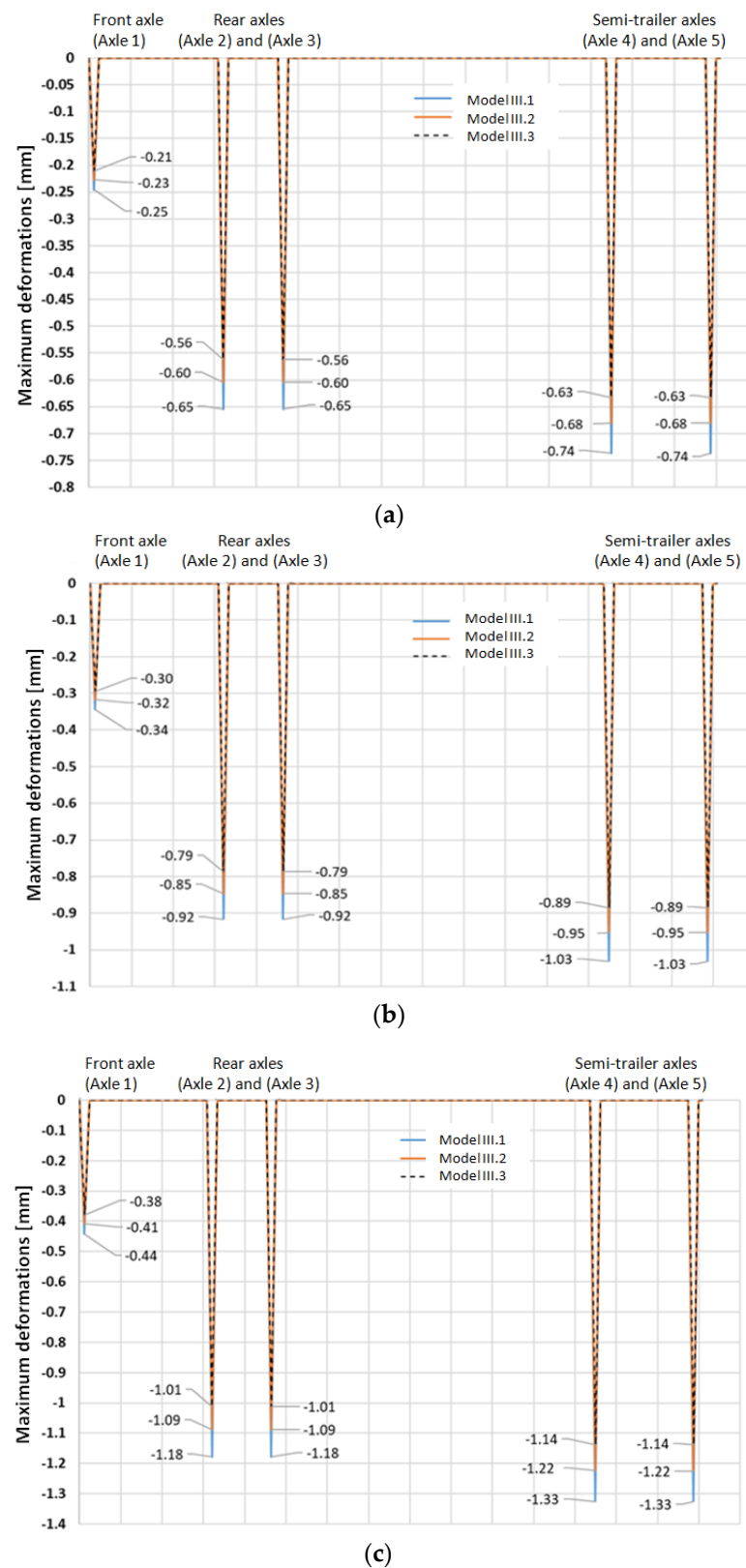


Figure 15. The maximum deformations recorded at type III road systems loaded at 25 tons (a), 35 tons (b) and 45 tons (c).

Compared to the deformations recorded for the type of road systems required at 25, 35 and 45 t loads, it was found that the maximum values were located in the middle of the pressure surface, varying depending on the axle that passes over the surface subjected at

pressure. Thus, it was observed that regardless of the road system and load, the lowest values appear in the case of the front axle (Table 4), after which the deformations increase in the case of the rear axles and reach maximum values in the case of the semi-trailer's axles, when the deformations tend to be three times higher than those recorded at the front wheels.

Table 4. The maximum deformations recorded in road systems subjected at 25, 35 and 45 tons.

		Maximum Deformations (mm)								
		Front Axle			Rear Axle			Semi-Trailer's Axles		
Type of structure		I.1	I.2	I.3	I.1	I.2	I.3	I.1	I.2	I.3
Loading (tons)	25	0.21	0.19	0.18	0.56	0.51	0.48	0.62	0.58	0.53
	35	0.29	0.27	0.25	0.78	0.72	0.67	0.87	0.81	0.75
	45	0.37	0.35	0.32	1.00	0.92	0.86	1.12	1.04	0.96
Type of structure		II.1	II.2	II.3	II.1	II.2	II.3	II.1	II.2	II.3
Loading (tons)	25	0.25	0.22	0.21	0.66	0.60	0.55	0.74	0.67	0.62
	35	0.35	0.31	0.29	0.92	0.84	0.77	1.04	0.94	0.86
	45	0.45	0.40	0.37	1.19	1.08	0.98	1.34	1.21	1.11
Type of structure		III.1	III.2	III.3	III.1	III.2	III.3	III.1	III.2	III.3
Loading (tons)	25	0.25	0.23	0.21	0.65	0.60	0.56	0.74	0.68	0.63
	35	0.34	0.32	0.30	0.92	0.85	0.79	1.03	0.95	0.89
	45	0.44	0.41	0.38	1.18	1.09	1.01	1.33	1.22	1.14

Comparing the maximum deformations recorded for those nine variants of road systems subjected to tests (Table 4), it could be observed that equal or very close values appear between type II and III road systems, which were composed of three layers, and not of four, as occurs in the case of type I structure. Regardless of the loading level (25, 35 or 45 t) and the ballast layer's thickness on the embankment (200, 300 or 400 mm), the type I recorded the lowest values of the maximum deformations, which indicates that the broken stone layer sort 63/90 (150 mm) and the optimum mix ballast layer (100 mm) play an important role in their behavior. In addition, for all types of road systems, the maximum deformations recorded were smaller as the ballast layer on the embankment was thicker, which makes the structure more difficult to deform due to increased stiffness.

3.2.3. The Residual Deformations Recorded at 25, 35 and 45 Tons

Type I Road Systems

From the analysis of Figure 16a–c, it could be seen that, regardless of the loading level, the residual deformations in the case of type I road systems were greater when the ballast layer's thickness on the embankment was smaller (I.1). This was due to the elasticity of this structure compared to types I.2 and I.3, where the ballast layer's thickness was greater and stiffened the structure, making it better resist the loading forces that tend to deform it.

Compared to the impact of the loading on the same type of road system (I.1, I.2 or I.3—Figure 16a–c), it was found that there were significant increases between the residual deformations resulting from loadings of 25 and 35 t (0.136 mm—I.3 and 0.162 mm—I.1); and from 35 to 45 t increases occur, the residual deformations increasing by 0.181 mm (I.3) and 0.218 mm (I.1) at 45 t loadings compared to those recorded at 35 t.

Type II Road Systems

Figure 17a–c illustrates the residual deformations in the case of type II road systems, subjected at 25, 35 and 45 t. As in the case of type I, in the case of type II a greater elasticity of the road system with a smaller thickness (II.1) could be seen, the residual deformations being greater in the structures that have a layer of ballast on the embankment of greater thickness (II.2 and II.3). On the other hand, a significant increase in the residual deformations from the 25 t to the 35 t loadings was also observed (0.199 mm—II.3 and 0.254 mm—II.1). In the case of increasing the loading level, from 35 to 45 t, a significant

increase in the residual deformations was observed, the values increasing by 0.245 mm at II.3, respectively by 0.338 mm at II.1.

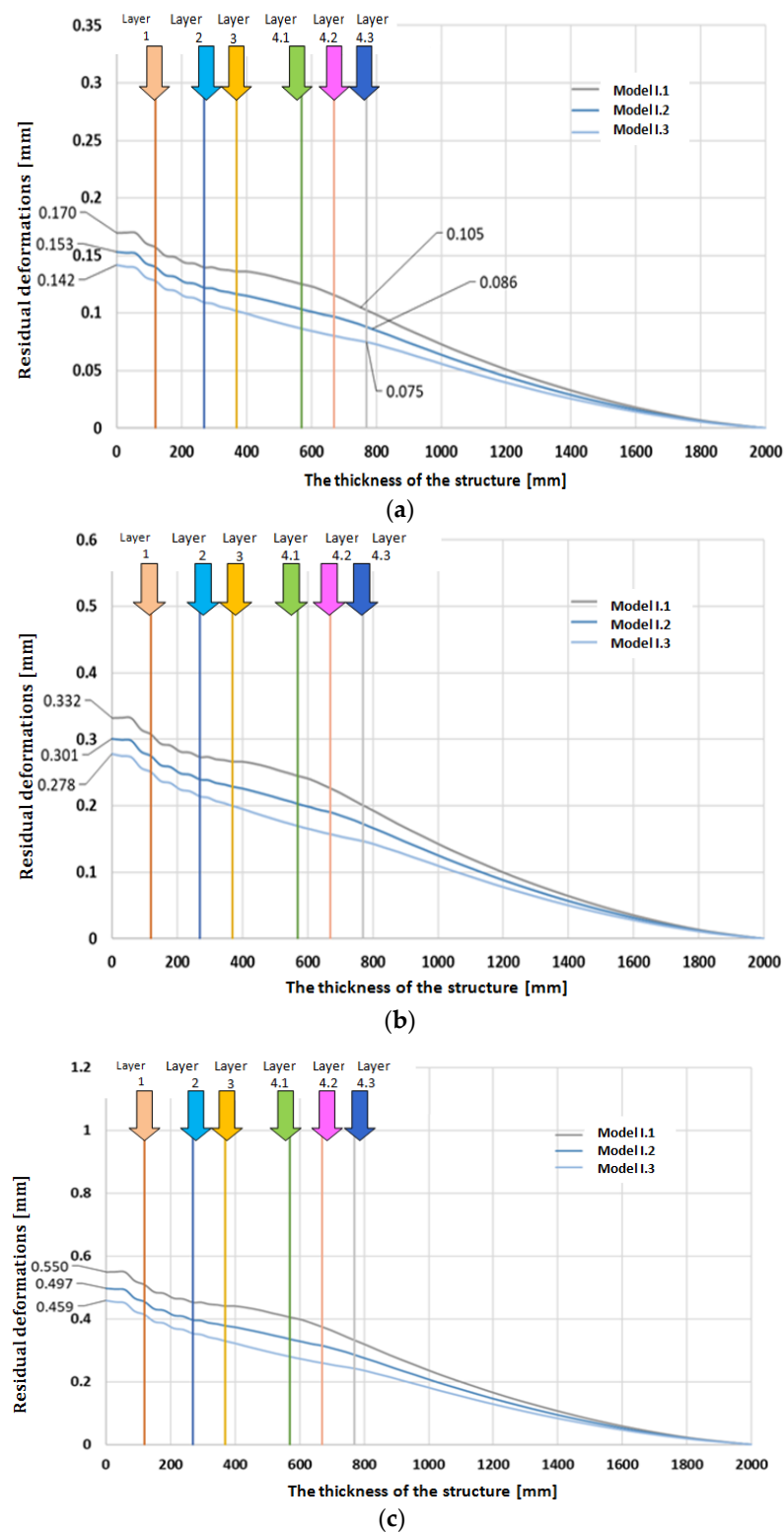
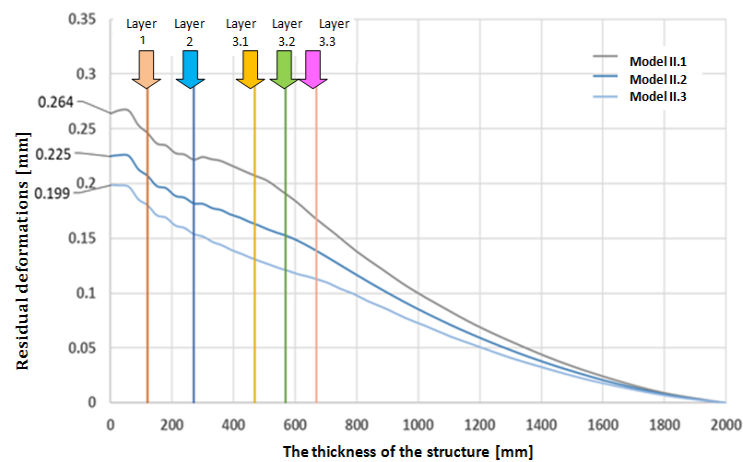
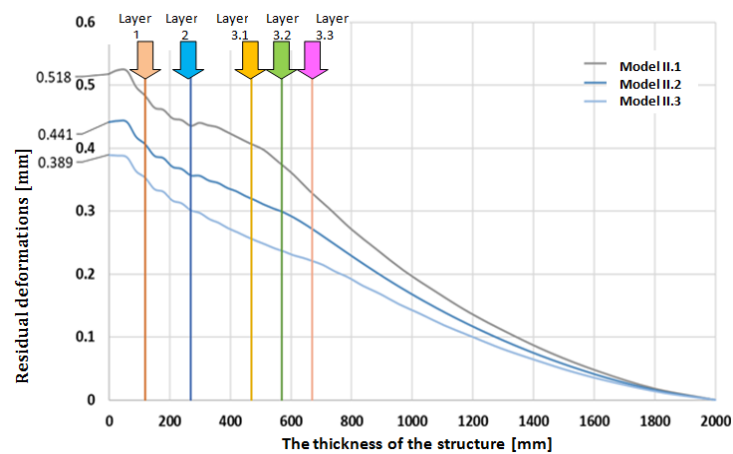


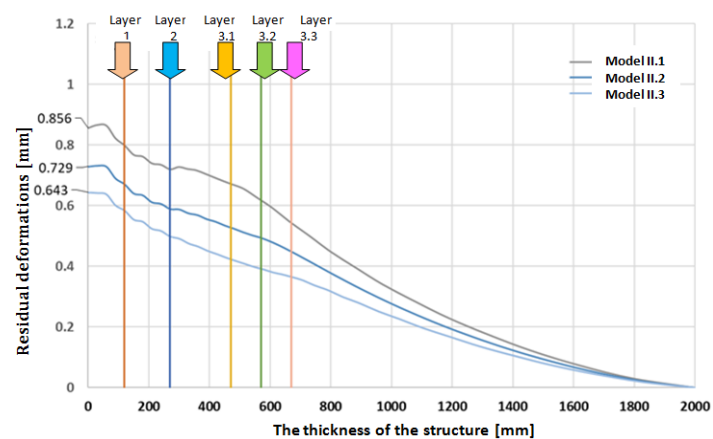
Figure 16. The residual deformations recorded at the type I road systems subjected at 25 tons (a), 35 tons (b) and 45 tons (c).



(a)



(b)



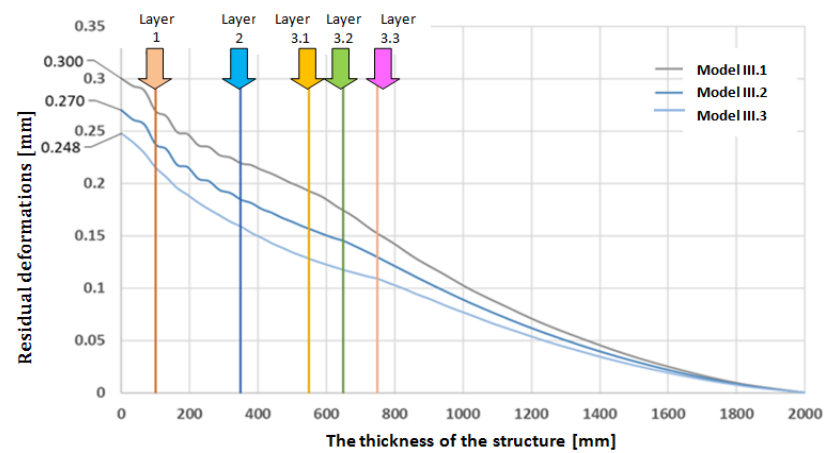
(c)

Figure 17. The residual deformations recorded at the type II road systems subjected at 25 tons (a), 35 tons (b) and 45 tons (c).

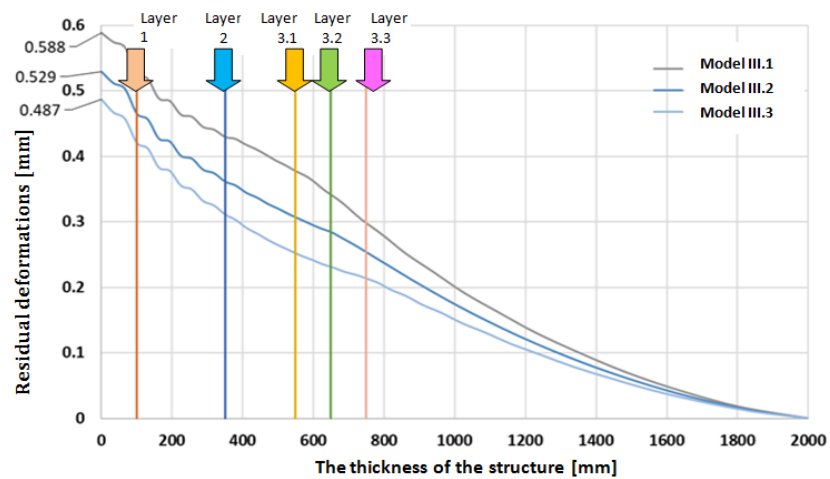
Type III Road Systems

The tendency to increase the residual deformations in the case of road systems with a thinner layer of ballast was found in type III road systems (Figure 18a–c), the most elastic, regardless of the level of loading, being the III.1 structures, where the residual deformation oscillates between 0.300 mm at 25 t loads and 0.972 at 45 t loads. Furthermore, the tendency

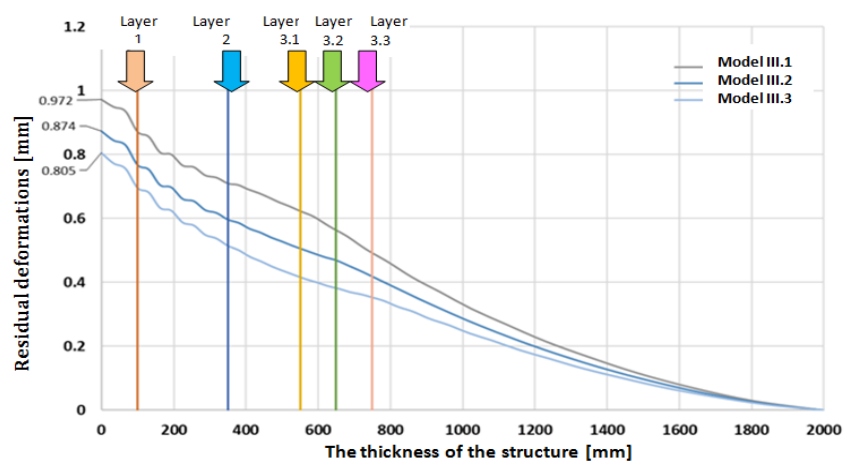
to decrease the size of the residual deformations with the increase in the thickness of the ballast layer at the level of the embankment was also observed.



(a)



(b)



(c)

Figure 18. The residual deformations recorded at the type III road systems subjected at 25 tons (a), 35 tons (b) and 45 tons (c).

The impact of the loading level was even more obvious in the case of type III road systems. Thus, unlike the residual deformations recorded at 25 t, increases of 0.239 mm (III.3) and 0.288 mm (III.1) were observed with the increase in load at 35 t, respectively by 0.318 mm (III.3) and 0.384 mm (III.1) when the residual deformations resulting from the loadings of 35 and 45 t were taken into consideration.

The comparative analysis of the residual deformations, specific to the road systems analyzed and subjected to 25, 35 and 45 tons loads (Table 5), highlights the significant impact that the road system's thickness, the number of layers, and the materials that enter into their composition play in stiffening them. Regardless of the loading and the road system's type (I, II or III), it could be observed that the residual deformations were greater when the thickness of the structure was smaller. On the other hand, it was found that type I road system show less residual deformations than type II and III, an aspect that can be attributed to the two layers in their composition (the crushed stone layer sort 63/90—150 mm and the optimal ballast layer—100 mm), which gives the structures better resistance to loadings which try to deform them.

Table 5. Residual deformations recorded at 25, 35 and 45 tons loadings.

Loading [tons]	25 tons			35 tons			45 tons		
Type I road systems	I.1	I.2	I.3	I.1	I.2	I.3	I.1	I.2	I.3
Residual deformations [mm]	0.170	0.153	0.142	0.332	0.301	0.278	0.550	0.497	0.459
Type II road systems	II.1	II.2	II.3	II.1	II.2	II.3	II.1	II.2	II.3
Residual deformations [mm]	0.264	0.225	0.199	0.518	0.441	0.389	0.856	0.729	0.643
Type III road systems	III.1	III.2	III.3	III.1	III.2	III.3	III.1	III.2	III.3
Residual deformations [mm]	0.300	0.270	0.248	0.588	0.529	0.487	0.972	0.874	0.805

4. Discussion

The behavior of road systems, when they are made in accordance with the standards [54], depends on the load level of the vehicle and the speed with which it moves with the load [14], the responses to dynamic loadings being much more pronounced compared to those from static loads, these effects rise with the increase in the vehicle's speed [60]. In the present study, the maximum deformation always occurs in the center of the pressing surface, an observation which was made by the Marko and his collaborators [82], as well as by the Leonardi and his collaborators [76].

Regarding the distribution of loads on the axles, the research of various authors [17,60,61,74] have once again highlighted their importance, especially since vehicles of high tonnage, which have the load distributed on several axles, subject the roads at very high unit pressures [5,12,54], the stress induced on the road structures being different depending on the loadings on each axis separately [61]. From this point of view, the obtained results indicate that the maximum deformations, for the considered ATF-25 forest truck, always occur at the double rear axle, the road systems deforming more with increasing the total loading of the vehicle (25, 35 and 45 tons). This is fully justified in the case of round wood transport, of large sizes. In the Regulations for the design of forest roads, in force [15], as well as in other specialist books [22,23] it was mentioned that the length of such trucks can reach up to 16.5 m (including the load), which means that a good part of the load is distributed on the rear axle and the semi-trailer axles. Due to the constructive variant of the ATF-25 forest truck, the lowest values of the maximum deformations appear at the front axle, a situation found in three-axle garbage trucks, which Chen and his collaborators [61] referred to.

Comparing the results for the three analyzed parameters (maximum deformation, the displacement into the depth of the entire road system and residual deformation) it was found that one of the main influencing factors was the road system's thickness, which can stiffen the structure or make it more elastic, as it emerged from the research carried out by Trzinski and Kaczmarzyk [54], which compares road systems of different thicknesses. In addition, the layers of the road system have a significant influence on

the analyzed parameters, both through their thickness and through the stony materials used. They must have good resistance to weathering, friction and erosion and be able to interlock well enough to resist traffic loadings that tend to dislodge them, thereby creating permanent degradation and deformation in the structure [59]. In this sense, type I road systems, composed of three layers (370 mm), to which a layer of ballast was added on the embankment (200, 300 or 400 mm), show better values for the three analyzed parameters, compared to the other types of road systems (II and III), even if, in the end, the values are influenced by the thickness of the ballast layer.

Comparing the values obtained for the displacements of the layers into depth, it was found that they have close or even equal values for types II and III road systems, a fact that can be attributed to the similarities between these road systems, composed of three layers of stony materials, the differences being only in the thickness of the layers and not in the type of stone materials (mixed crushed stone, pitching of crushed stone and ballast). In this regard, Trzcinski and Kaczmarzyk [54] state that the lack of differences between the deformation modules at different thicknesses of the road systems can be attributed to other factors, such as the particularities of the earth in the embankment and the road execution method, but not to the loadings or materials which enter in the road systems composition. On the other hand, the same authors [54] state that the greatest increase in deformations, with the increase in loading, was observed in road systems made up of a single layer of gravel, with a thickness of 12–15 cm. The authors [54] also stated the fact that road systems with two layers (gravel and broken stone), used for secondary forest roads in Romania, were characterized by a greater deformation in the case of poor quality embankments, which is why other authors [21] recommend that, in order to support loads that are expected to travel on a road, road systems should be placed on embankments with high bearing capacity, especially since the stress caused by traffic loads affects each layer differently, including the earth in the embankment [11].

5. Conclusions

1. In the present study, the maximum deformation always occurs in the center of the pressing surface;
2. The deformation of the roadbed depends on the road system composition (as a number of layers), its deformation being various for each case studied;
3. A higher road system's thickness can reduce the displacement into the depth of the layers and the maximum deformations;
4. Among all nine types of road systems evaluated, it was observed that type III road systems was the most rigid, and it had the smallest deformations at the level of the contact surface, a fact due to the ballast layer's thickness;
5. In all the road systems studied, the largest deformations occur at the semi-trailer axles, the values being higher when the road system is of less thickness, and the loading is higher;
6. By verifying the nine variants of standard road systems at loadings of 25, 35 and 40 tons, it was found that not all of them provide the necessary bearing capacity for the current traffic imposing themselves, as the case may be, increasing the thickness of system's layers.

Author Contributions: Conceptualization E.-C.M. and I.B.; methodology, I.B.; software, I.B.; validation, I.B.; formal analysis, I.B.; investigation, I.B.; resources, E.-C.M.; data curation, E.-C.M.; writing—original draft preparation, E.-C.M.; writing—review and editing, E.-C.M.; visualization, E.-C.M. and I.B.; supervision, E.-C.M.; project administration, E.-C.M.; funding acquisition, E.-C.M. and I.B. All authors have read and agreed to the published version of the manuscript.

Funding: This research received no external funding.

Institutional Review Board Statement: Not applicable.

Informed Consent Statement: Not applicable.

Data Availability Statement: Not applicable.

Acknowledgments: The authors thank to the Transilvania University of Brasov and to the National Forest Administration RNP-ROMSILVA; for all the support provided, the information made available and the particularly important suggestions.

Conflicts of Interest: The authors declare no conflict of interest.

References

- Kochenderfer, J.N.; Wendel, G.W.; Clay Smith, H. *Cost of and Soil Loss on "Minimum-Standard" Forest Truck Road Constructed in the Central Appalachians*; Research paper NE-544; United State Department of Agriculture, Forest Service, Northeastern Forest Experiment Station: Broomall, PA, USA, 1984; 12p.
- Legea nr. 10 din 18 Ianuarie 1995 (Republicată) Privind Calitatea în Construcții. Published in the Official Monitor of Romania no.765 of 30 September 2016. Available online: <https://legislatie.just.ro/Public/DetaliuDocument/5729> (accessed on 30 August 2022).
- Alexandru, V. *Construcția și Întreținerea Drumurilor Forestiere*; Infomarket Press: Brasov, Romania, 2000; 397p.
- Normativ pentru Reabilitarea Drumurilor Forestiere. RD-001-11. Emitted by the Minister of the Environment and Forests no. 1373 on 4 May 2012. 34p. Available online: <http://apepaduri.gov.ro/wp-content/uploads/2014/07/Cuprins-Normativ-reabilitare-1.pdf> (accessed on 7 March 2019).
- Mușat, E.C.; Alexandru, V.M.; Ciobanu, V.D.; Săceanu, S.C.; Antoniadă, C.; Vișan, J. The type and the extension of degradations caused by the introduction in the timber transportation of the increased weight vehicles. *Rev. Pădurilor* **2014**, *5–6*, 38–43.
- Săceanu, S.C. Contribuții privind Comportarea Drumurilor Forestiere în Condițiile Extinderii Transportului Lemnului cu Autovehicule de Tonaj Sporit. Ph.D. Thesis, Transilvania University of Brasov, Brasov, Romania, 2014.
- Antoniadă, C.C. Contribuții Privind Majorarea Capacității Portante a Drumurilor Forestiere, în Vederea Extinderii Transportului Lemnului cu Autovehicule de Tonaj Sporit. Ph.D. Thesis, Transilvania University of Brasov, Brasov, Romania, 2015.
- Kharavassefat, P.; Jelagin, D.; Birgisson, B. Dynamic response of flexible pavements at vehicle-road interaction. *Road Mater. Pavement Des.* **2015**, *16*, 256–276. [[CrossRef](#)]
- Kharavassefat, P.; Jelagin, D.; Birgisson, B. The non-stationary response of flexible pavements to moving loads. *Int. J. Pavement Eng.* **2016**, *17*, 458–470. [[CrossRef](#)]
- Research Report 148: *Infrastructure: Road Construction Cost on Infrastructure Procurement Benchmarking: 2017 Update*; Australian Government, Department of Infrastructure, Regional Development and Cities, Bureau Infrastructure, Transport and Regional Economics: Canberra, Australia, 2018; 54p.
- Akgul, M.; Akburak, S.; Yurtseven, H.; Akay, A.O.; Cigizoglu, H.K.; Demir, M.; Ozturk, T.; Eksi, M. Potential impacts of weather and traffic conditions on road surface performance in terms of forest operations continuity. *Appl. Ecol. Environ. Res.* **2019**, *17*, 2533–2550. [[CrossRef](#)]
- Bitir, I.; Mușat, E.C.; Derczeni, R.A.; Ciobanu, V.D. The influence of the increased tonnage upon the superstructure of forest roads. In Proceedings of the 19th International Multidisciplinary Scientific Geoconference SGEM 2019, Albena, Bulgaria, 28 June–7 July 2019.
- Bitir, I.; Mușat, E.C.; Lunguleasa, A.; Ciobanu, V.D. Monitoring the transport on the Ciobănuș forest road within the Bacău Forestry Department. *Recent J.* **2021**, *1*, 10–16. [[CrossRef](#)]
- Kosztka, M.; Markó, G.; Péterfalvi, J.; Primusz, P.; Tóth, C. Measuring bearing capacity on forest roads in Hungary. In *A Magyar Tudományok Akadémia Agrártudományok Osztálya*; Nyugat-Magyarországi Egyetem: Gödöllő, Hungary, 2008.
- Normativ privind Proiectarea Drumurilor Forestiere. Indicativ PD-003-11. Emitted by the Minister of the Environment and Forests no.1374 on 4 May 2012. 34p. Available online: <http://apepaduri.gov.ro/wp-content/uploads/2014/07/Cuprins-Normativ-proiectare-1.pdf> (accessed on 7 March 2019).
- Mușat, E.C.; Ciobanu, V.D.; Vișan, J.; Antoniadă, C.; Săceanu, S.C. Analiza variantelor de structuri rutiere în contextul sporirii capacității portante a drumurilor forestiere. *Rev. Pădurilor* **2016**, *3–4*, 91–99.
- Zhu, X.Q.; Law, S.S. Recent development in inverse problems of vehicle-bridge interaction dynamics. *J. Civ. Struct. Health Monit.* **2016**, *6*, 107–128. [[CrossRef](#)]
- Constantinescu, Ș.; Suci, D. Strategii de întreținere și reparații pentru structuri rutiere la drumuri noi. *Rev. Drumuri Poduri* **2002**, *67*, 13–17.
- Șerbulea, M. Certificarea de conformitate a calității produselor. Calitatea construcțiilor. Legea 10/18 ianuarie 1995. *Rev. Drumuri Poduri* **2002**, *65*, 31–33.
- Grajewski, S.M.; Czerniak, A.; Kuroska, E.E. The influence of vegetation succession on bearing capacity of forest roads made of unbound aggregates. *Forests* **2020**, *11*, 1137. [[CrossRef](#)]
- Yorulmaz, A.; Sivrikaya, O.; Uysal, F. Evaluation of the bearing capacity of poor subgrade soils stabilized with waste marble powder according to curing time and freeze-thaw cycles. *Arab. J. Geosci.* **2021**, *14*, 360. [[CrossRef](#)]
- Olteanu, N. *Drumuri Forestiere. Proiectare*; Transilvania University Press: Brasov, Romania, 1995; 173p.
- Olteanu, N. *Proiectarea Drumurilor Forestiere*; Lux Libris Press: Brasov, Romania, 1996; 236p.
- Olsson, L.; Lohmander, P. Optimal forest transportation with respect to road investments. *Forest Policy Econ.* **2005**, *7*, 369–379. [[CrossRef](#)]

25. Li, L.; Sandu, C. On the impact of cargo weight, vehicle parameters, and terrain characteristics on the prediction of traction for off-road vehicles. *J. Terramechanics* **2002**, *44*, 221–238. [[CrossRef](#)]
26. Zanoncio, A.J.V.; Carvalho, A.G.; da Silva, M.G.; Lima, J.T. Importance of wood drying to the forest transport and pulp mill supply. *Cerne* **2017**, *23*, 147–152. [[CrossRef](#)]
27. Pentek, T.; Pičman, D.; Potočnik, I.; Dvorščak, P.; Nevečerel, H. Analysis of an existing forest road network. *CROJFE* **2005**, *26*, 39–50.
28. Enache, A.; Stampfer, K.; Ciobanu, V.; Brânzea, O.; Duță, C. Forest road network planning with state of the art tools in a private forest district from Lower Austria. *BUT–Ser. II* **2011**, *4*, 33–40.
29. Trzcinski, G.; Kozakiewicz, P.; Selwakowski, R. The technical aspects of using timber in the construction of forest roads. *J. Water Land Dev.* **2017**, *34*, 241–247. [[CrossRef](#)]
30. Derczeni, R.A.; Salcă, E.A.; Ciobanu, D.V.; Bitir, I.; Mușat, E.C. Research on establishing criteria for calculating the tax/road tolling for vehicles used for timber transport on forest roads. In Proceedings of the International Symposium “Forest and Sustainable Development”—The 8th Edition, Brasov, Romania, 25–27 October 2018.
31. Southworth, J.; Tucker, C. The influence of accessibility, local institution and socioeconomic factors on forest cover change in the mountains of Western Honduras. *MRD* **2001**, *21*, 276–283. [[CrossRef](#)]
32. Popovici, V.; Bereziuc, R.; Clinciu, I. Extinderea rețelei de drumuri pentru accesibilizarea fondului forestier și, în general, a pădurii. *Bucov. For.* **2003**, *XI*, 36–40.
33. Navarro Maroto, P.J.; Rodriques Bayo, J.; Codina i Palou, M.; Dominquez i Tores, G.; Lopes Vicens, Y. *Prospects for the Market Supply of Wood and Other Forest Products from Areas with Fragmented Forest Ownership Structure*; Task II. Case Study: Catalonia, Spain; Centre Tecnologic Forestal de Catalunya: Catalunya, Spain, 2010; 93p.
34. Bereziuc, R.; Alexandru, V.; Ciobanu, V.; Mușat, E.C.; Dumitrașcu, A.-E.; Antoniadă, C.; Vișan, J. The density index of the forest road network managed by the National Forest Administration (R.N.P.). In Proceedings of the International Conference “Forest and Sustainable Development”, Brasov, Romania, 25–26 October 2014.
35. Bereziuc, R. Realizări și perspective în domeniul căilor forestiere de transport. *An. Univ. “Ștefan Cel Mare” Suceava* **2004**, *2*, 9–14.
36. Potočnik, I.; Pentek, T.; Pičman, D. Impact of traffic characteristics on forest roads due to forest management. *CROJFE* **2005**, *26*, 51–57.
37. Grulois, S.; Pellegrini, M.; Lingua, E.; Grignolato, S.; Protti, F.; Vitali, A.; Rebolj, L.; Grum, A.; Ginot, C.; Corette, T.; et al. General presentation of the wood transport sector in the alpine space. *Interreg. Alp. Space Proj.* **2014**, *29*.
38. Turk, Y. Construction method of forest roads in Turkey. In Proceedings of the 5th Forest Engineering Conference—FORMEC, Gerard, France, 23–26 September 2014.
39. De Clercq, E.M.; De Wulf, R.; Van Herzele, A. Relating spatial pattern of forest cover to accessibility. *Landsc. Urban Plan.* **2007**, *80*, 14–22. [[CrossRef](#)]
40. Huan, R.; Yeh, C. Development of an assessment framework for green highway construction. *J. Chin. Inst. Eng.* **2008**, *31*, 573–585. [[CrossRef](#)]
41. Krč, J.; Beguš, J. Planning forest opening with forest roads. *CROJFE* **2013**, *34*, 217–228.
42. Cebon, D. *Interaction between Heavy Vehicles and Roads*; SAE Technical Paper 930001; 1993; 81p. [[CrossRef](#)]
43. Lachini, E.; Fiedler, N.; Silva, G.; Pinheiro, C.; Carmo, F. Operational analysis of forestry transportation using self-loading trucks in a mountainous region. *For. Ambient.* **2018**, *25*, e20150060. [[CrossRef](#)]
44. Layton, D.A.; LeDoux, C.B.; Hassler, C.C. *Cost Estimators for Construction of Forest Roads in Central Appalachians*; Research Paper NE-665; United State Department of Agriculture, Forest Service, Northeastern Forest Experiment Station: Morgantown, WV, USA, 1992; 8p.
45. Asikainen, A. Simulation of logging and barge transport of wood from forests on islands. *Int. J. For. Eng.* **2001**, *12*, 43–50. [[CrossRef](#)]
46. Akay, A.E. Minimizing total costs of forest roads with computer-aided design model. *Asdhana* **2006**, *31*, 621–633. [[CrossRef](#)]
47. Lindström, J.; Fjeld, D. Routing of self-loading logging trucks in Sweden. In Proceedings of the 34th Council on Forest Engineering, Quebec, QC, Canada, 12–15 June 2011.
48. Ghajar, I.; Nakafi, A.; Karimimajd, A.M.; Boston, K.; Torabi, S.A. A program for cost estimation of forest road construction using engineer’s method. *Forest Sci. Technol.* **2013**, *9*, 111–117. [[CrossRef](#)]
49. Acuna, M. Timber and biomass transport optimization: A review of planning issue, solution techniques and decision support tools. *CROJFE* **2017**, *38*, 279–290.
50. Olteanu, I.; Stan, I. Transportul auto forestier—prezent și viitor. *Rev. Pădurilor* **1992**, *107*, 43–48.
51. Holzleitner, F.; Kanzian, C.; Stampfer, K. Analyzing time and fuel consumption in road transport of round wood with an onboard fleet manager. *Eur. J. Forest Res.* **2011**, *130*, 293–301. [[CrossRef](#)]
52. Ordonanța nr. 43 din 28 August 1997 privind Regimul Drumurilor. Emitted by the Romanian Govern and Published in the Official Monitor no. 237 on 29 June 1998. Available online: <https://legislatie.just.ro/Public/DetaliiDocument/11269> (accessed on 30 August 2022).
53. Bereziuc, R.; Alexandru, V.; Ciobanu, V.; Ignea, G. *Elemente de Fundamentare a Normativului de Proiectare a Drumurilor Forestiere*; Transilvania University Press: Brasov, Romania, 2008.
54. Trzcinski, G.; Kaczmarzyk, S. Estimation of carrying capacity of slag and gravel forest road pavements. *CROJFE* **2006**, *27*, 27–36.

55. Rahbarisakht, S.; Hadi Moayeri, M.; Hayati, E.; Moein Sadeghi, S.M.; Kepfer-Rojas, S.; Hadi Pahlavani, M.; Kappel Schmidt, I.; Borz, S.A. Changes in soil's chemical and biochemical properties induced by road geometry in the Hyrcanian temperate forests. *Forest* **2021**, *12*, 1805. [[CrossRef](#)]
56. Begus, J.; Pertlik, E. *Guide for Planning, Construction and Maintenance of Forest Roads*; FAO: Budapest, Hungary, 2017; 51p.
57. Normativ privind Proiectarea și Execuția Împietruirilor Drumurilor de Pământ. Condiții de calitate. Indicativ AND-582/2002. *Buletin Tehnic Rutier* **2002**, *3*, 7–58.
58. Bereziuc, R.; Alexandru, V.; Ciobanu, V. Accesibilizarea Pădurilor în Condiții Ecologice, în Vederea Valorificării Masei Lemnoase. *Rev. Pădurilor* **2013**, *128*, 28–34.
59. Tahvanainen, T.; Anttila, P. Supply chain cost analysis of long-distance transportation of energy wood in Finland. *Biomass Bioenerg.* **2011**, *35*, 3360–3375. [[CrossRef](#)]
60. Beskou, N.D.; Hatzigeorgiou, G.; Theodorakopoulos, D. Finite element inelastic analysis of 3-D flexible pavements under moving loads. In Proceedings of the COMPDYN 2015—5th ECCOMAS Thematic Conference on Computational Methods in Structural Dynamics and Earthquake Engineering, Crete Island, Greece, 25–27 May 2015.
61. Chen, Y.; Zhang, H.; Zhu, X.; Liu, D.W. The response of pavement to the multi-axle vehicle dynamic load. In Proceedings of the International Conference of Electrical, Automation and Mechanical Engineering—EAME, Phuket, Thailand, 26–27 July 2015.
62. Ciobanu, V.D. Cercetări Privind Utilizarea Geogriurilor la Consolidarea Părții Carosabile a Drumurilor Forestiere Amplasate în Terenuri Argiloase. Ph.D. Thesis, Transilvania University of Brașov, Brașov, Romania, 1998.
63. Yanov, D.V.; Zelepugin, S.A. Road pavement design using the finite element method. *CICMCM—IOP Conf. Ser. J. Phys. Conf. Ser.* **2019**, *1214*, 012024. [[CrossRef](#)]
64. Rodgers, M.; Hayes, G.; Healy, M.G. Cyclic loading tests on sandstone and limestone shale aggregates used in unbound forest roads. *Constr. Build. Mater.* **2009**, *23*, 2421–2427. [[CrossRef](#)]
65. Ryan, T.; Phillips, H.; Ramsay, J.; Dempsey, J. *Forest Road Manual. Guidelines for the Design, Construction and Management of Forest Roads*; COFORD, National Council for Forest Research and Development Agriculture Building: Dublin, Ireland, 2004; 156p.
66. Kapoor, K.; Prozzi, J.A. *Methodology for Quantifying Pavement Damage Caused by Different Axle and Load Configurations*; Report SWUTC/05/167827-1, April 2005; Center for Transportation Research, University of Texas: Austin, TX, USA, 2005.
67. Thom, N. *Principles of Pavement Engineering*, 2nd ed.; ICE Publishing: London, UK, 2014; 456p.
68. Bereziuc, R. *Drumuri Forestiere*; Didactical and Pedagogical Press: Bucharest, Romania, 1981; 335p.
69. Arnold, G.K. *Rutting of Granular Pavements*. Ph.D. Thesis, University of Nottingham, Nottingham, UK, 2004.
70. Thyagarajan, S. Improvements to Strain Computation and Reliability Analysis of Flexible Pavements in the Mechanical-Empirical Pavement Design Guide. Ph.D. Thesis, Washington State University, Washington, DC, USA, 2009.
71. Calvarano, L.S.; Leonardi, G.; Palamara, R. Finite element modeling of unpaved road reinforced with geosynthetics. *Procedia Eng.* **2017**, *189*, 99–104. [[CrossRef](#)]
72. Karadag, H.; Firat, S.; Isik, N.S.; Yilmaz, G. Determination of permanent deformation of flexible pavements using finite element model. *Gradevinar* **2022**, *74*, 471–480. [[CrossRef](#)]
73. Harvey, J.B. A Large Displacement Finite Element Analysis of a Reinforced Unpaved Road. Ph.D. Thesis, University of Oxford, Oxford, UK, 1986.
74. Rahmani, M.; Kim, Y.R.; Park, Y.B.; Jung, J.S. Mechanistic analysis of pavement damage and performance prediction based on finite element modeling with viscoelasticity and fracture of mixtures. *LHI J. Land Hous. Urban Aff.* **2020**, *11*, 95–104.
75. Ambassa, Z.; Allou, F.; Petit, C.; Eko, R. Fatigue life prediction of an asphalt pavement subjected to multiple axle loadings with viscoelastic FEM. *Constr. Build. Mater.* **2013**, *43*, 443–452. [[CrossRef](#)]
76. Leonardi, G.; Lo Bosco, D.; Palamara, R.; Suraci, F. Finite element analysis of geogrid-stabilized unpaved roads. *Sustainability* **2020**, *12*, 1929. [[CrossRef](#)]
77. Sawan, A.M.M.I. Finite Elements Performance Analysis of Asphalt Pavement Mixtures Modified Using Nano-Additives. Master's Thesis, The Higher Institute of Engineering, El-Shorouk Academy, Cairo, Egypt, 2013.
78. Mulungye, R.M.; Owende, P.M.O.; Mellon, K. Finite element modelling of flexible pavements on soft soil subgrades. *Mater. Des.* **2007**, *28*, 739–756. [[CrossRef](#)]
79. Barksdale, R.D. Performance of crushed-stone base courses. *Transp. Res. Rec.* **1984**, *954*, 78–87.
80. Liang, P.; Yang, Y.; Huang, H.; Liu, J.; Guo, N. Experimental study on fractal characteristics of particle size distribution by repeated compaction of road recycling crushed stone. *Appl. Sci.* **2021**, *12*, 10303. [[CrossRef](#)]
81. *Rural Road Manual. Indian Roads Congress Special Publication 20*; The Indian Roads Congress: New Delhi, India, 2002; 383p.
82. Markó, G.; Primusz, P.; Péterfalvi, J. Measuring the bearing capacity of forest roads with an improved Benkelman beam apparatus. *Acta Silv. Lignaria Hung.* **2013**, *9*, 97–110. [[CrossRef](#)]